12-2015

The Performance of Quaternary Amplitude Modulation with Quaternary Spreading in the Presence of Interfering Signals

Allison Manhard
Clemson University, amanhar@g.clemson.edu

The Performance of Quaternary Amplitude Modulation with Quaternary Spreading in the Presence of Interfering Signals

---

A Thesis
Presented to
the Graduate School of
Clemson University

In Partial Fulfillment
of the Requirements for the Degree
Master of Science
Electrical Engineering

---

by
Allison Ann Manhard
December 2015

Accepted by:
Dr. Daniel Noneaker, Committee Chair
Dr. Harlan Russell
Dr. Carl Baum

Abstract

Multiple-access digital communications is considered with direct-sequence spread-spectrum (DS-SS) quadrature amplitude modulation and quaternary spreading in each transmission. Each transmitted signal undergoes attenuation and a delay at a receiver in the additive white Gaussian noise channel. The receiver uses coherent demodulation with a correlation detector synchronized to the one of the K received signals so that the $K-1$ other transmissions act as interference.

The average probability of error at the output of the detector is determined using Monte Carlo simulation and compared with an approximation in which the interference component in each detection statistic is approximated by a Gaussian random variable. Closed-form expressions are derived for the first and second moments of the interference under several circumstances. The moments are used with the "Gaussian approximation", and the accuracy of the approximation is investigated for each of the circumstances.

Table of Contents

Title Page . . . . . **i**

List of Figures . . . . . **iv**

1 Introduction **1**

2 System Model **4**
2.1 Transmitter 4
2.2 Channel 9
2.3 Receiver 10
2.4 Measures of Signal Quality and System Performance 11
2.5 Statistical Model of System 12

3 Characterization of the Decision Statistics **14**
3.1 Interference with a Fixed Delay and Phase Offset 19
3.2 Symbol-Synchronous Interference 21
3.3 Uniformly Distributed Interference Delays 22

4 Performance Evaluation and Approximation **25**
4.1 Closed-form expressions for the Gaussian Approximation 25
4.2 QPSK with Symbol Synchronous Inference 28
4.3 QPSK and Interference with a Fixed Delay 28
4.4 QPSK with a Random Interference Delay 29
4.5 M-QAM with Symbol Synchronous Inference 30
4.6 M-QAM and Interference with a Fixed Delay 32
4.7 M-QAM with a Random Interference Delay 33

5 Conclusion **35**

Appendices **36**
A Conditional Joint Distribution of Key Auxiliary Random Variables 37
B Characterization of Multiple-Access Interference 39
C Moments of Interference Terms With Random Signature Sequences 46

Bibliography **48**

List of Figures

2.1 System model. 5
2.2 Block diagram of system. 6
2.3 Transmitter model. 7
2.4 Constellation diagram for QPSK. 7
2.5 Constellation diagram for 16-QAM. 8
2.6 Illustration of DS-SS modulation. 9
2.7 Channel model. 10
2.8 Receiver model. 11

4.1 Probability of error for QPSK with two users and various values of N. 29
4.2 Probability of bit error for QPSK with various phases of interferer, $K = 2, N = 8$, and an SIR of 0 dB. 30
4.3 Probability of bit error for QPSK with $K = 2$, various interference delays, $N = 8$, and an SIR of 0 dB. 31
4.4 Probability of bit error for QPSK with random interference delay, $K = 2$, $N = 8$, and an SIR of 0 dB. 31
4.5 Probability of error for 16-QAM, chip and symbol synchronous, $K = 2$ and various values of N. 32
4.6 Probability of symbol error for 16-QAM with $K = 2$, various interference delays, and an SIR of 0 dB. 33
4.7 Probability of symbol error for 16-QAM with random interference delay, $K = 2$, $N = 32$, and an SIR of 0 dB. 34

Chapter 1

Introduction

Direct-sequence spread-spectrum (DS-SS) multiple-access communications [1] is a widely used modulation format for both commercial cellular communications and military tactical radio communications. Among the advantages of DS-SS multiple-access communications is the ability to tolerate denser reuse of each portion of the frequency spectrum across a wide-area radio network compared with time-division multiple-access or frequency-division multiple-access. It is achieved at the cost of vulnerability to power mismatches in the multiple transmitted signals at a given receiver, and under normal operation, the performance is often limited by the effect of multiple-access interference on the detection of the information contained in the transmission of interest to the receiver. Thus accounting for the effect of multiple-access interference is key to an accurate analysis of the system's performance.

Analysis of the performance of a link in a DS-SS multiple-access communication system is complicated by the complexity of accounting precisely for the effect of multiple interferers on the desired signal at a receiver. Precise evaluation leads to complex analytical expressions which require computationally intensive evaluation, and the alternative of Monte Carlo simulation of system performance similarly requires significant computation. The cost of this complexity is compounded if high-fidelity link performance results are desired for use in the simulation of a large network of radios.

The computation required for link performance modeling is reduced substantially if the system model is modified to approximate the effect of interfering signals on the desired signal by imposing an appropriately chosen Gaussian distribution on the component of the receiver's decision

statistic that represents the effect of the interferers. This "Gaussian approximation" [1] leads to a performance evaluation whose accuracy depends on the particular circumstances considered and the assumptions used in the approximation. Numerous methods have been introduced to improve the tradeoff between the accuracy of the computational burden of the approximation (such as [2] and [3]). Most have focused on a system in which each transmitter employs DS-SS binary phase-shift-keyed (BPSK) modulation, DS-SS quaternary phase-shift-keyed (QPSK) modulation, or DS-SS offset QPSK (OQPSK) modulation.

In this thesis, we consider the performance of a multiple-access communication system in which each transmitter uses DS-SS M-ary quadrature amplitude modulation (M-QAM) with distinct spreading sequences in the inphase and quadrature signals. Each transmitted signal uses the same modulation format and signal parameters, each one undergoes an arbitrary channel attenuation, delay, and carrier phase shift in propagating to the receiver of interest, and the sum of the resulting signals are corrupted by additive white Gaussian noise at the receiver. The receiver uses coherent demodulation with inphase and quadrature correlators synchronized to the inphase and quadrature spreading signals of the desired signal, respectively. The $K-1$ other transmissions thus act as interference to the detection of the information in the desired signal. The receiver uses zero-threshold, matched-filter detection of each channel symbol in the inphase and quadrature signals.

The average probability of error in the detection of a data symbol or the probability of error in detecting a bit of information is determined using Monte Carlo simulation. The error probability is compared with an approximation in which the effect of the multiple-access interference on detection is approximated by the effect of a Gaussian random variable with the same first and second moments as the multiple-access interference. Closed-form expressions are derived for the first and second moments of the interference under several circumstances for use with the "Gaussian approximation", extending previous results for DS-SS BPSK modulation [4] and DS-SS OQPSK modulation [5] . The accuracy of the approximation is investigated for each of the circumstances.

The model of the DS-SS M-QAM multiple-access system is defined in Chapter 2. Closed-form expressions are derived in Chapter 3 and the appendices for the first and second moments of the terms in the decision statistics which are due to the presence of multiple-access interference at the receiver. Expression are developed for several circumstances of interest. The moments are used to determine Gaussian approximations to the interference terms in the decision statistics and the resulting probability of symbol-detection error and probability of bit error. The probability

of error under the Gaussian approximation is compared in Chapter 4 to the actual probability of error (obtained by Monte Carlo simulation) for each circumstance of interest. The accuracy of the approximations is summarized in Chapter 5.

Chapter 2

System Model

The communication system considered in the thesis consists of K transmitted signals over an additive white Gaussian noise (AWGN) channel, using quaternary data modulation and quaternary direct-sequence spreading, as shown in Figures 2.1 and 2.2. Each transmitted signal represents a different information source. The signal is attenuated and delayed by the channel between the corresponding transmitter and the receiver, and the received signal consists of the sum of the attenuated, delayed signals corrupted by an AWGN random process. The receiver converts the received signal into an inphase (I) statistic and quadrature (Q) statistic for each transmitted data symbol in the desired signal. The two statistics are applied to a decision device that determines the corresponded detected data symbol. We consider one of the signals to be the signal of interest, and the other $K-1$ signals are considered as interfering signals. The receiver is designed to detect the information represented by the signal of interest.

2.1 Transmitter

The transmitter for the kth signal in the communication system is represented in Figure 2.3. Each transmitted signal has an inphase and a quadrature component and two bit streams that are spread by respective spreading sequences. The information source generates a sequence of information bits $\underline{b}_k$ which are mapped to data symbols, with the ith output of the mapper consists of the data symbol represented by the pair of real values $(u_{k,i}, v_{k,i})$.

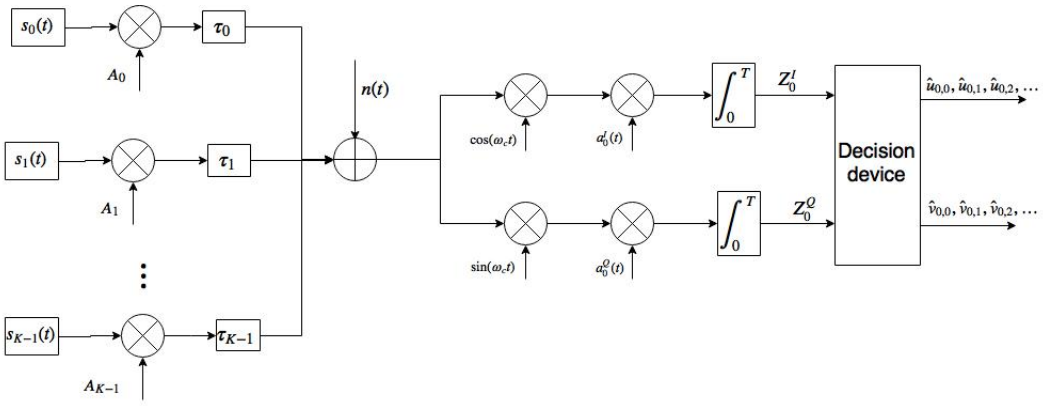

Figure 2.1: System model.

2.1.1 Data Signals

The modulation format we consider is rectangular, symmetric M-ary quadrature amplitude modulation(M-QAM) [6] in which each of $u_{k,i}$ and $v_{k,i}$ is taken from the set $\left\{\pm 1, \pm 3, \ldots, \pm\sqrt{M}-1\right\}$ where M is the size of the symbol set. The ith pair of data symbols determines the polarities of inphase and quadrature data signals over the time interval $[iT, (i+1)T)$, where T is the *symbol duration*. The data signals for transmitter k are given by

$$w_k^I(t) = \sum_{i=-\infty}^{\infty} u_{k,i} p_T(t - iT) \tag{2.1}$$

and

$$w_k^Q(t) = \sum_{i=-\infty}^{\infty} v_{k,i} p_T(t - iT). \tag{2.2}$$

2.1.1.1 QPSK Data Signal

We consider quadrature phase-shift keying (QPSK) [6] as an example of M-QAM where $M = 4$ and all symbols in the set have the same magnitude. The inphase and quadrature symbols $u_{k,i}$ and $v_{k,i}$ are chosen from the set $\{+1, -1\}$. We can represent the symbols in the constellation diagram shown in Figure 2.4. Since there are four symbols in the symbol set, each symbol represents two bits of information. The constellation shown in this figure uses Gray coding [6] as the mapping from information bits to data symbols, so that nearest-neighbor symbols differ by only one information bit.

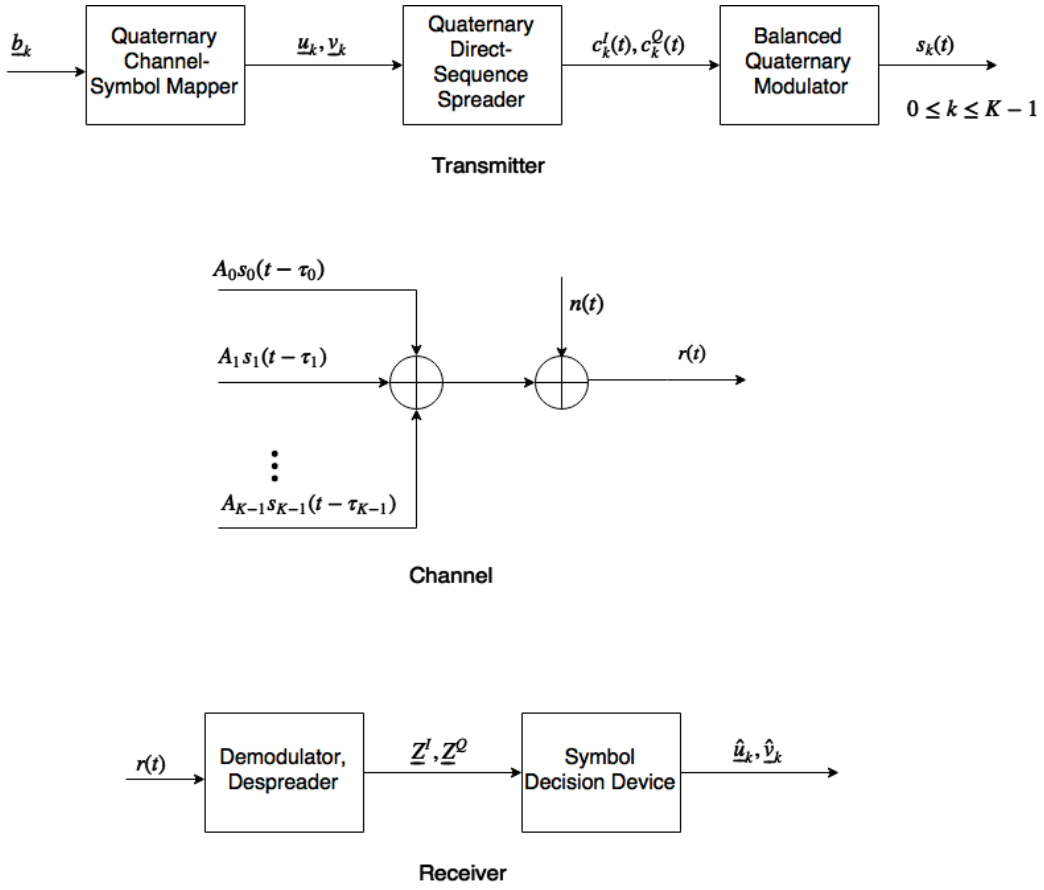

Figure 2.2: Block diagram of system.

2.1.1.2 16-QAM Data Signal

Another example signal set we consider is 16-QAM, in which the inphase and quadrature components are chosen from the set $\{-3, -1, +1, +3\}$. This is illustrated in the constellation diagram in Figure 2.5. For this symbol set, each symbol represents four bits of information, and Gray coding is used for bit assignments.

2.1.2 Direct-Sequence Spread-Spectrum Data Signals

Spread-spectrum modulation increases the bandwidth of a signal in a manner which can be exploited by the receiver to mitigate the effects of multipath propagation and interference from other users of the channel. One form of spread spectrum is direct-sequence spread-spectrum (DS-SS) modulation. DS-SS makes us of a pseudo-random sequence of pulses that are much shorter than the symbol duration. The duration of each pulse is known as the *chip duration*. This is illustrated in

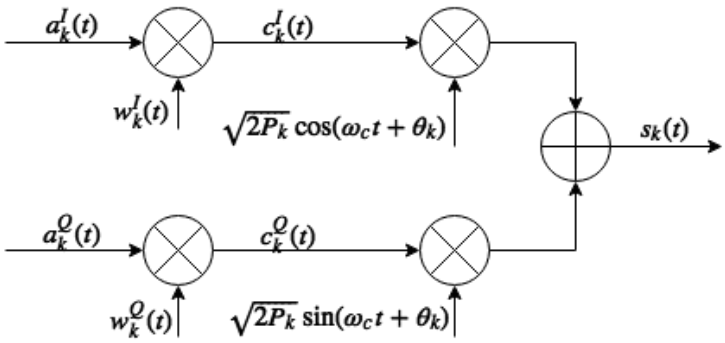

Figure 2.3: Transmitter model.

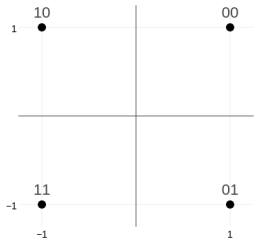

Figure 2.4: Constellation diagram for QPSK.

Figure 2.6.

The spreading signals in the inphase and quadrature channels for transmitted signal k are given by

$$a_k^Q(t) = \sum_{j=-\infty}^{\infty} a_{k,j}^Q \psi_c(t - jT_c) \tag{2.3}$$

and

$$a_k^I(t) = \sum_{j=-\infty}^{\infty} a_{k,j}^I \psi_c(t - jT_c), \tag{2.4}$$

respectively, where $a_{k,i}^I, a_{k,i}^Q \in \{-1, 1\}$, T_c is the chip duration, and $\psi_c(t)$ is the chip waveform with an average power of one. I.e.

$$\frac{1}{T_c}\int_0^{T_c} \psi_c^2(t)dt = 1. \tag{2.5}$$

The *spreading factor* is given by $N = \frac{T}{T_c}$, where N is assumed to be an integer. The *signature sequences* of the kth transmitted signal for the inphase and quadrature channels, $\{a_{k,i}^I\}$ and $\{a_{k,i}^Q\}$, respectively, are defined by a sequence of elements from the set $\{-1, +1\}$. The data signals defined in

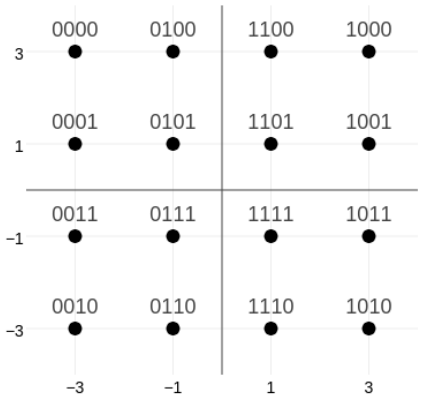

Figure 2.5: Constellation diagram for 16-QAM.

equations (2.1) and (2.2) are multiplied with the spreading signal to form the inphase and quadrature DS-SS data signals

$$c_k^I(t) = a_k^I(t) w_k^I(t) \tag{2.6}$$

and

$$c_k^Q(t) = a_k^Q(t) w_k^Q(t), \tag{2.7}$$

respectively.

2.1.3 Transmitted Signal

The transmitted M-QAM signal is formed by modulation of inphase and quadrature sinusoidal carriers by the inphase and quadrature DS-SS data signals, respectively. The kth transmitted signal is given by

$$s_k(t) = \sqrt{2P_k} c_k^I(t) \cos(\omega_c t + \theta_k) + \sqrt{2P_k} c_k^Q(t) \sin(\omega_c t + \theta_k), 0 \le k \le K-1, \tag{2.8}$$

where ω_c is the angular frequency, θ_k is the carrier phase, and $c_k^I(t)$ and $c_k^Q(t)$ are as defined in equations (2.6) and (2.7), respectively. The transmitted power in each of the inphase and quadrature components of $s_k(t)$ during the ith symbol interval are given by $P_k u_{k,i}^2$ and $(P_k v_{k,i}^2$, respectively.

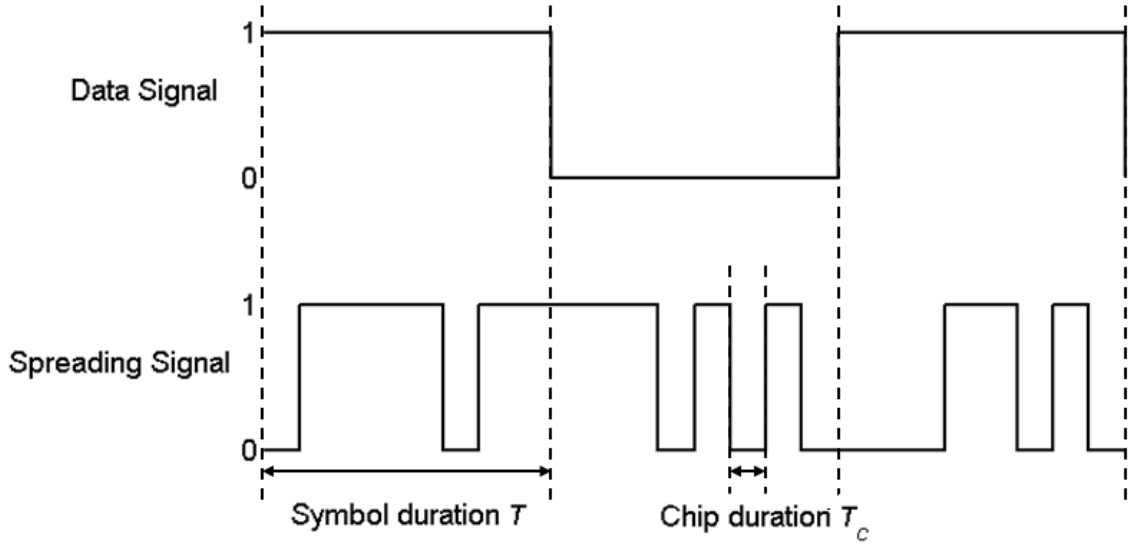

Figure 2.6: Illustration of DS-SS modulation.

For the special case of QPSK modulation ($M = 4$), the transmitted power in each component is P_k regardless of the data symbol in the symbol interval. In comparison, offset QPSK (OQPSK) modulation is considered in [5] in which the kth transmitted signal is given by

$$s_k(t) = \sqrt{2P_k}c_k^I\left(t - \frac{T_c}{2}\right)\cos\left(\omega_c t + \theta_k\right) + \sqrt{2P_k}c_k^Q\left(t\right)\sin\left(\omega_c t + \theta_k\right), 0 \leq k \leq K-1. \tag{2.9}$$

2.2 Channel

The channel over which the signal is transmitted is an AWGN channel with $K-1$ interfering signals, where $n(t)$ is an AWGN process with two-sided power spectral density $N_0/2$. The kth transmitted signal is attenuated by the multiplicative factor A_k and delayed by τ_k at the receiver. The channel is shown in Figure 2.7. The received signal thus is given by

$$r(t) = \sum_{k=0}^{K-1} A_k\sqrt{2P_k}c_k^I\left(t-\tau_k\right)\cos\left(\omega_c t + \Phi_k\right) + \sum_{k=0}^{K-1} A_k\sqrt{2P_k}c_k^Q\left(t-\tau_k\right)\sin\left(\omega_c t + \Phi_k\right) + n(t) \tag{2.10}$$

where $\Phi_k = \Theta_k - \omega_c\tau_k$ is the accumulated carrier phase at the receiver for the kth signal.

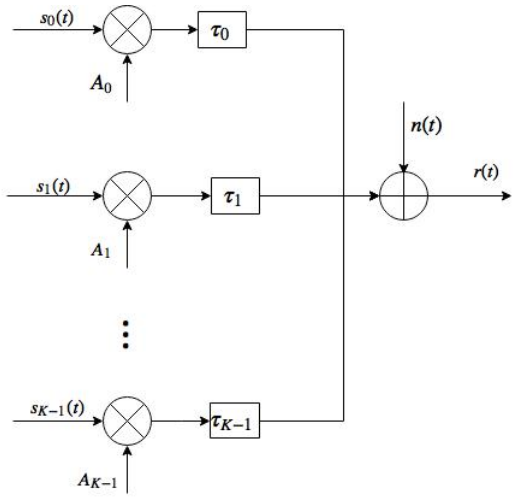

Figure 2.7: Channel model.

2.3 Receiver

A block diagram of the receiver is shown in Figure 2.8. Without loss of generality, we consider a receiver designed to detect the information from transmitter zero and its detection of the data symbol transmitted over the symbol interval $[0, T)$. Also, without loss of generality, we assume that $\tau_0 = 0$ and $\Phi_0 = 0$. The receiver uses coherent demodulation with inphase and quadrature correlators synchronized to the inphase and quadrature spreading signals of the desired signal, respectively. It is assumed that the receiver has a local reference that is matched to the phase of the desired component of the received signal, it has a perfect estimate of the symbol timing of the desired component of the desired component of the received signal, and for $M > 4$, it has a perfect estimate of the power in the desired component of the received signal for each data symbol in the signal constellation. The latter permits the receiver to set the thresholds for the decision regions of the decision device that yield maximum-likelihood symbol detection if the signal is corrupted by AWGN [6]. The inphase decision statistic can be written as

$$Z^I = \int_0^T r(t) a_0^I(\tau) \cos(\omega_c \tau) d\tau. \tag{2.11}$$

The quadrature decision statistic can be similarly written as

$$Z^Q = \int_0^T r(t) a_0^Q(\tau) \sin(\omega_c \tau) d\tau. \tag{2.12}$$

The decision statistics can be represented as

$$Z^I = S^I + \eta^I + \sum_{k=1}^{K-1} I_k^I = S^I + N^I \tag{2.13}$$

and

$$Z^Q = S^Q + \eta^Q + \sum_{k=1}^{K-1} I_k^Q = S^Q + N^Q \tag{2.14}$$

where S^I is the contribution from the desired signal, η^I is the contribution from the noise, $\sum_{k=1}^{K-1} I_k^I$ is the contribution from the interfering signals, and I_k^I is the interference component in the inphase subchannel from the kth signal, $1 \leq k \leq K-1$. The components S^Q, η^Q, and I_k^Q, $1 \leq k \leq K-1$, are similarly defined for the quadrature subchannel.

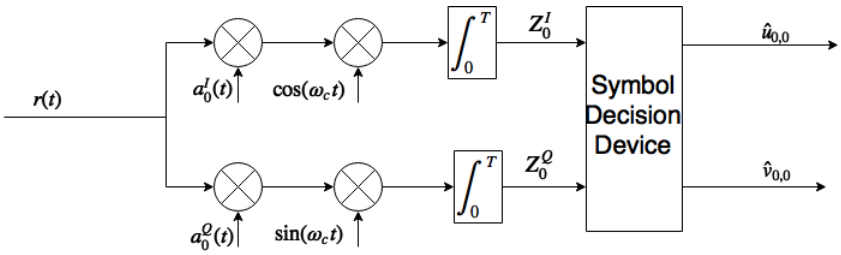

Figure 2.8: Receiver model.

2.4 Measures of Signal Quality and System Performance

Three measures of the quality of the received signal are used in this thesis. The *signal-to-interference-plus-noise ratio* (SINR) at the receiver accounts for the effect of both the thermal noise and interfering signals on the detection of the desired signal. For a given set of data symbols,

$$\underline{U} = \{u_{1,-1}, u_{1,0}, \ldots, u_{K-1,-1}, u_{K-1,0}\} \tag{2.15}$$

and

$$\underline{V} = \{v_{1,-1}, v_{1,0}, \ldots, v_{K-1,-1}, v_{K-1,0}\} \tag{2.16}$$

in the interfering signals, the SINR is given by

$$\Gamma(\underline{U}, \underline{V}) = \frac{A_0^2 P_0 T^2}{\text{Var}\left(N^I(\underline{U}, \underline{V})\right) + \text{Var}\left(N^Q(\underline{U}, \underline{V})\right)}. \tag{2.17}$$

The *signal-to-noise ratio* (SNR) can be expressed in terms of the average energy per data symbol at the receiver, E_s, or the average energy per bit of information at the receiver. From equation (2.17) and [6], the former is given by $\frac{E_s}{N_0} = \frac{M-1}{3}\Gamma(\underline{0}, \underline{0})$ and the latter is given by

$$\frac{E_b}{N_0} = \frac{M-1}{3\log_2(M)}\Gamma(\underline{0}, \underline{0}). \tag{2.18}$$

The average *signal-to-interference ratio* (SIR) at the receiver is the ratio of the average power in the desired signal to the sum of the average power in the interfering signals. Since all transmissions use the same modulation format with equally likely data symbols, the SIR is given by

$$\Lambda = \frac{A_0^2 P_0}{\sum_{k=1}^{K-1} A_k^2 P_k}. \tag{2.19}$$

Two measures of system performance are considered in the thesis: the (average) probability of symbol error, P_s, and the (average) probability of bit error, P_b. Since non-binary modulation is considered, $P_b \neq P_s$. In general, the probability of bit error depends on the mapping of the information bits to code symbols used by the transmitter.

2.5 Statistical Model of System

All the analysis and examples in subsequent chapters assume the same joint statistics for the random variables that determine the transmitted signals. The data symbols, $u_{k,i}$ and $v_{k,i}$ are uniformly distributed over the set $\left\{\pm 1, \pm 3, \ldots, \pm\sqrt{M} - 1\right\}$ where M is the size of the symbol set. The chip polarities, $a_{k,i}^I$ and $a_{k,i}^Q$, have values in $\{-1, 1\}$ with

$$\Pr(u_{k,i} = 1) = \Pr(v_{k,i} = 1) = \Pr(a_{k,i}^I = 1) = \Pr(a_{k,i}^Q = 1) = \frac{1}{2} \tag{2.20}$$

for $0 \leq k \leq K-1$ and all i. The random variables that determine the transmitted signals over the interval of interest are mutually independent.

Two scenarios are considered in subsequent chapters with respect to the effect of the channel on the interfering signals. In the first scenario, the delay of the kth transmitted signal, τ_k, and its accumulated phase at the receiver, Φ_k, are fixed for $1 \leq k \leq K-1$. In the second scenario, the delay is uniformly distributed on the interval $[0, T)$ and the phase is uniformly distributed on the interval $[0, 2\pi)$ for $1 \leq k \leq K-1$. The $2(K-1)$ random variables $\{\tau_k, \Phi_k\}$, $1 \leq k \leq K-1$ are mutually independent and independent of the set of data-symbol and chip polarity random variables. The noise random process $n(t)$ is independent of the random variables that determine the transmitted signals.

Chapter 3

Characterization of the Decision Statistics

In this chapter, we consider the decision statistics for the system in Chapter 2, and we develop expressions for their first and second moments for several conditions of interest. The development is modeled after the development in [5] (which in turn draws on results from [4]). Binary PSK and OQPSK DS-SS signals are considered in [4] and [5], respectively. In this chapter, we adapt the approach of [5] to DS-SS QAM signals.

The inphase correlator statistic for the desired signal $s_0(t)$ is given in equations (2.11) and (2.13), and the quadrature correlator statistic is given in equations (2.12) and (2.14). In all that follows, conditioning on $u_{0,0}, v_{0,0}$ and the signature sequences of the desired signal is implicit. The respective expected values of the desired portion of the inphase and quadrature components of the decision statistic are given as

$$S^I = u_{0,0} A_0 T \sqrt{\frac{P_0}{2}} \tag{3.1}$$

and

$$S^Q = v_{0,0} A_0 T \sqrt{\frac{P_0}{2}}. \tag{3.2}$$

The noise components of both the inphase decision statistic and the quadrature decision statistic

have a mean of zero, and their respective variances are given by

$$\sigma^2_{\eta_0^I} = \sigma^2_{\eta_0^Q} = \frac{N_0 T}{4}. \tag{3.3}$$

The component of the inphase decision statistic due to the kth interfering signal can be written as

$$I_k^I = W_k^I A_k \sqrt{\frac{P_k}{2}} \tag{3.4}$$

where

$$W_k^I = U_k^I \cos(\Phi_k) - V_k^I \sin(\Phi_k), \tag{3.5}$$

$$U_k^I = \int_0^T c_k^I(t-\tau_k) a_0^I(t) dt, \tag{3.6}$$

and

$$V_k^I = \int_0^T c_k^Q(t-\tau_k) a_0^I(t) dt. \tag{3.7}$$

Similarly, for the quadrature decision statistic,

$$I_k^Q = W_k^Q A_k \sqrt{\frac{P_k}{2}} \tag{3.8}$$

where

$$W_k^Q = U_k^Q \cos(\Phi_k) - V_k^Q \sin(\Phi_k), \tag{3.9}$$

$$U_k^Q = \int_0^T c_k^Q(t-\tau_k) a_0^Q(t) dt, \tag{3.10}$$

and

$$V_k^Q = \int_0^T c_k^I(t-\tau_k) a_0^Q(t) dt. \tag{3.11}$$

The random variables U_k^I, V_k^I, U_k^Q and V_k^Q can be expressed in terms of the chip-pulse continuous partial autocorrelation functions and the discrete cross-correlation functions of the spreading sequence of the desired signal and the spreading sequence of the kth interfering signal [5]. The ran-

dom variable U_k^I is expanded as

$$U_k^I = \sum_{i=0}^{N-2} H_{k,i}^I \left[\hat{R}_{\psi_c}(S_k) + a_{0,i}^I a_{0,i+1}^I R_{\psi_c}(S_k) \right] + H_{k,N-1}^I \hat{R}_{\psi_c}(S_k) + H_{k,N}^I R_{\psi_c}(S_k), \tag{3.12}$$

where

$$H_{k,i}^I = \begin{cases} u_{k,-1} a_{k,i-\gamma_k}^I a_{0,i}^I, & \text{if } 0 \le i \le \gamma_k - 1 \\ u_{k,0} a_{k,i-\gamma_k}^I a_{0,i}^I, & \text{if } \gamma_k \le i \le N-1 \\ u_{k,-1} a_{k,-\gamma_k-1}^I a_{0,0}^I, & \text{if } i = N. \end{cases} \tag{3.13}$$

The chip-pulse continuous partial autocorrelation functions are given by

$$R_{\psi_c}(s) = \int_0^s \psi_c(t)\psi_c(t + T_c - s)dt \tag{3.14}$$

and

$$\hat{R}_{\psi_c} = \int_0^{T_c - s} \psi_c(t)\psi_c(t - s)dt, \tag{3.15}$$

and the *chip delay* random variable is given by $S_k = \tau_k - \gamma_k T_c$, with $\gamma_k = \lfloor \tau_k / T_c \rfloor$. The subsequent development is conditioned on τ_k (and thus, γ_k) except where otherwise noted. We assume $0 \le \tau_k < T$ for $1 \le k \le K-1$, which is general for the distributions specified in Section 2.5. Similarly, the random variable V_k^I is expanded as

$$V_k^I = \sum_{i=0}^{N-2} \tilde{H}_{k,i}^I \left[\hat{R}_{\psi_c}(S_k) + a_{0,i}^I a_{0,i+1}^I R_{\psi_c}(S_k) \right] + \tilde{H}_{k,N-1}^I \hat{R}_{\psi_c}(S_k) + \tilde{H}_{k,N}^I R_{\psi_c}(S_k), \tag{3.16}$$

where

$$\tilde{H}_{k,i}^I = \begin{cases} v_{k,-1} a_{k,i-\gamma_k}^Q a_{0,i}^I, & \text{if } 0 \le i \le \gamma_k - 1 \\ v_{k,0} a_{k,i-\gamma_k}^Q a_{0,i}^I, & \text{if } \gamma_k \le i \le N-1 \\ v_{k,-1} a_{k,-\gamma_k-1}^Q a_{0,0}^I, & \text{if } i = N. \end{cases} \tag{3.17}$$

For the quadrature decision statistic, the random variable U_k^Q is expanded as

$$U_k^Q = \sum_{i=0}^{N-2} H_{k,i}^Q \left[\hat{R}_{\psi_c}(S_k) + a_{0,i}^Q a_{0,i+1}^Q R_{\psi_c}(S_k) \right] + H_{k,N-1}^Q \hat{R}_{\psi_c}(S_k) + H_{k,N}^Q R_{\psi_c}(S_k), \tag{3.18}$$

where

$$H_{k,i}^{Q} = \begin{cases} v_{k,-1} a_{k,i-\gamma_k}^{Q} a_{0,i}^{Q}, & \text{if } 0 \le i \le \gamma_k - 1 \\ v_{k,0} a_{k,i-\gamma_k}^{Q} a_{0,i}^{Q}, & \text{if } \gamma_k \le i \le N-1 \\ v_{k,-1} a_{k,-\gamma_k-1}^{Q} a_{0,0}^{Q}, & \text{if } i = N. \end{cases} \tag{3.19}$$

Similarly, the random variable V_k^Q is expanded as

$$V_k^Q = \sum_{i=0}^{N-2} \tilde{H}_{k,i}^{Q} \left[\hat{R}_{\psi_c}(S_k) + a_{0,i}^{Q} a_{0,i+1}^{I} R_{\psi_c}(S_k) \right] + \tilde{H}_{k,N-1}^{I} \hat{R}_{\psi_c}(S_k) + \tilde{H}_{k,N}^{Q} R_{\psi_c}(S_k), \tag{3.20}$$

where

$$\tilde{H}_{k,i}^{Q} = \begin{cases} u_{k,-1} a_{k,i-\gamma_k}^{I} a_{0,i}^{Q}, & \text{if } 0 \le i \le \gamma_k - 1 \\ u_{k,0} a_{k,i-\gamma_k}^{I} a_{0,i}^{Q}, & \text{if } \gamma_k \le i \le N-1 \\ u_{k,-1} a_{k,-\gamma_k-1}^{I} a_{0,0}^{Q}, & \text{if } i = N. \end{cases} \tag{3.21}$$

In Appendix A, it is shown that the $(K-1)(N+1)$ sets of four random variables

$$\mathcal{H}_{k,i} = \left\{ H_{k,i}^{I}, \tilde{H}_{k,i}^{I}, H_{k,i}^{Q}, \tilde{H}_{k,i}^{Q} \right\}, 0 \le i \le N, 1 \le k \le K-1, \tag{3.22}$$

are conditionally mutually independent given $\mathcal{M} = \bigcup_{k=1}^{K-1} \mathcal{M}_k$, where

$$\mathcal{M}_k = \left\{ |u_{k,0}|, |u_{k,-1}|, |v_{k,0}|, |v_{k,-1}| \right\}, 1 \le k \le K-1, \tag{3.23}$$

and that the conditioning for $\mathcal{H}_{k,i}$, $0 \le i \le N$ can be reduced to $\mathcal{M}_k$ for each k. The set of random variables $\left\{ H_{k,i}^{I}, \tilde{H}_{k,i}^{I}, H_{k,i}^{Q}, \tilde{H}_{k,i}^{Q} \right\}$ are shown to be conditionally dependent given $\mathcal{M}_k$, however, and some pairs of the random variables are conditionally correlated. The random variables $\left\{ U_k^I, V_k^I, U_k^Q, V_k^Q \right\}$ are shown in Appendix B to have a conditional mean of zero given $\mathcal{M}_k$. Their conditional second moments given $\mathcal{M}_k$ are also derived in Appendix B.

Now consider the expectation of the multiple-access interference with respect to uniformly distributed signature sequences for the desired signal. In Appendix C, it is shown that under this expectation,

$$\mathrm{E}\left[W_k^I | \mathcal{M}_k \right] = \mathrm{E}\left[W_k^Q | \mathcal{M}_k \right] = 0, \tag{3.24}$$

$$\begin{aligned}
\mathrm{E}\left[(W_k^I)^2|\mathcal{M}_k\right] = &\left[\gamma_k|u_{k,-1}|^2 + (N-\gamma_k)|u_{k,0}|^2\right]\hat{R}^2_{\psi_c}(S_k)\cos^2(\Phi_k) \\
&+ \left[(\gamma_k+1)|u_{k,-1}|^2 + (N-\gamma_k-1)|u_{k,0}|^2\right]R^2_{\psi_c}(S_k)\cos^2(\Phi_k) \\
&+ \left[\gamma_k|v_{k,-1}|^2 + (N-\gamma_k)|v_{k,0}|^2\right]\hat{R}^2_{\psi_c}(S_k)\sin^2(\Phi_k) \\
&+ \left[(\gamma_k+1)|v_{k,-1}|^2 + (N-\gamma_k-1)|v_{k,0}|^2\right]R^2_{\psi_c}(S_k)\sin^2(\Phi_k), \qquad (3.25)
\end{aligned}$$

$$\begin{aligned}
\mathrm{E}\left[(W_k^Q)^2|\mathcal{M}_k\right] = &\left[\gamma_k|v_{k,-1}|^2 + (N-\gamma_k)|v_{k,0}|^2\right]\hat{R}^2_{\psi_c}(S_k)\cos^2(\Phi_k) \\
&+ \left[(\gamma_k+1)|v_{k,-1}|^2 + (N-\gamma_k-1)|v_{k,0}|^2\right]R^2_{\psi_c}(S_k)\cos^2(\Phi_k) \\
&+ \left[\gamma_k|u_{k,-1}|^2 + (N-\gamma_k)|u_{k,0}|^2\right]\hat{R}^2_{\psi_c}(S_k)\sin^2(\Phi_k) \\
&+ \left[(\gamma_k+1)|u_{k,-1}|^2 + (N-\gamma_k-1)|u_{k,0}|^2\right]R^2_{\psi_c}(S_k)\sin^2(\Phi_k), \qquad (3.26)
\end{aligned}$$

and

$$\mathrm{E}\left[W_k^I W_k^Q|\mathcal{M}_k\right] = 0. \qquad (3.27)$$

For QPSK modulation, equations (3.25) and (3.26) simplify to

$$\mathrm{E}\left[(W_k^I)^2|\mathcal{M}_k\right] = \mathrm{E}\left[(W_k^Q)^2|\mathcal{M}_k\right] = N\left(\hat{R}^2_{\psi_c}(S_k) + R^2_{\psi_c}(S_k)\right). \qquad (3.28)$$

Note that the conditional first and second moments do not depend on Φ_k.

It is also shown in Appendix C that the $(K-1)$ sets $\left\{W_k^I, W_k^Q\right\}$ are conditionally uncorrelated given $\mathcal{M}$ and that conditioning for $\left\{W_k^I, W_k^Q\right\}$ can be reduced to $\mathcal{M}_k$ under expectation with respect to the uniformly distributed signature sequences of the desired signal. It follows that the $(K-1)$ sets $\{I_k^I, I_k^Q\}$, $1 \le k \le K-1$, are conditionally uncorrelated given $\mathcal{M}$ and that conditioning for $\{I_k^I, I_k^Q\}$ can be reduced to $\mathcal{M}_k$. Furthermore, from equations (3.5), (3.8), and (3.24) - (3.27), it follows that I_k^I and I_k^Q are conditionally uncorrelated, zero-mean random variables given $\mathcal{M}_k$ and

that

$$\begin{aligned}\mathrm{Var}\left(I_k^I|\mathcal{M}_k\right) =&\frac{A_k^2P_k}{2}\Big(\left[\gamma_k|u_{k,-1}|^2+(N-\gamma_k)|u_{k,0}|^2\right]\hat{R}^2_{\psi_c}(S_k)\cos^2(\Phi_k)\\&+\left[(\gamma_k+1)|u_{k,-1}|^2+(N-\gamma_k-1)|u_{k,0}|^2\right]R^2_{\psi_c}(S_k)\cos^2(\Phi_k)\\&+\left[\gamma_k|v_{k,-1}|^2+(N-\gamma_k)|v_{k,0}|^2\right]\hat{R}^2_{\psi_c}(S_k)\sin^2(\Phi_k)\\&+\left[(\gamma_k+1)|v_{k,-1}|^2+(N-\gamma_k-1)|v_{k,0}|^2\right]R^2_{\psi_c}(S_k)\sin^2(\Phi_k)\Big)\end{aligned}\tag{3.29}$$

and

$$\begin{aligned}\mathrm{Var}\left(I_k^Q|\mathcal{M}_k\right) =&\frac{A_k^2P_k}{2}\Big(\left[\gamma_k|v_{k,-1}|^2+(N-\gamma_k)|v_{k,0}|^2\right]\hat{R}^2_{\psi_c}(S_k)\cos^2(\Phi_k)\\&+\left[(\gamma_k+1)|v_{k,-1}|^2+(N-\gamma_k-1)|v_{k,0}|^2\right]R^2_{\psi_c}(S_k)\cos^2(\Phi_k)\\&+\left[\gamma_k|u_{k,-1}|^2+(N-\gamma_k)|u_{k,0}|^2\right]\hat{R}^2_{\psi_c}(S_k)\sin^2(\Phi_k)\\&+\left[(\gamma_k+1)|u_{k,-1}|^2+(N-\gamma_k-1)|u_{k,0}|^2\right]R^2_{\psi_c}(S_k)\sin^2(\Phi_k)\Big).\end{aligned}\tag{3.30}$$

Finally, from equations (2.13) and (2.14) and the definition of the system in Chapter 2, the random variables $\{\eta^I,\eta^Q\}$ are independent of $\{\mathcal{M}_k,I_k^I,I_k^Q\}$ and they are independent, zero-mean Gaussian random variables with

$$\mathrm{Var}(\eta^I)=\mathrm{Var}(\eta^Q)=\frac{N_0T}{4}.\tag{3.31}$$

3.1 Interference with a Fixed Delay and Phase Offset

The variance of each interference term is given by equations (B.6) and (B.13) above if the delay and phase offset of each interferer is fixed. We consider the special case of QPSK modulation first, then the general case of M-QAM.

3.1.1 QPSK with Fixed Delay and Phase Offset Interference

For QPSK modulation, $|u_{k,i}|=|v_{k,i}|=1$ for all k and i. In this section, two examples of chip waveforms are considered: the rectangular waveform and the raised-cosine waveform. For the

rectangular waveform, the chip autocorrelation functions are given by

$$R_{\psi_c}(s) = s \tag{3.32}$$

$$\hat{R}_{\psi_c}(s) = T_c - s. \tag{3.33}$$

Therefore the conditional variance of I_k can be written as

$$\begin{aligned}
\mathrm{Var}\left(I_k^I|\mathcal{M}_k\right) &= \mathrm{Var}\left(I_k^Q|\mathcal{M}_k\right) && (3.34)\\
&= \frac{A_k^2 P_k}{2} N\left(\hat{R}_{\psi_c}^2(S_k) + R_{\psi_c}^2(S_k)\right) && (3.35)\\
&= \frac{A_k^2 P_k}{2} N\left((T_c - S_k)^2 + (S_k)^2\right) && (3.36)\\
&= \frac{A_k^2 P_k}{2} N\left(T_c^2 - 2S_k T_c + 2S_k^2\right) && (3.37)
\end{aligned}$$

The energy per bit of information in the received signal is given by $E_b = A_0^2 T P_0$. From equations (2.17), (3.1), (3.2), (3.37), and (3.31), the SINR with a rectangular pulse waveform can be written as

$$\Gamma(\underline{U}, \underline{V}) = \left(\frac{N_0}{E_s} + \sum_{k=1}^{K-1} \frac{A_k^2 P_k}{N A_0^2 P_0}\left(1 - 2\frac{S_k}{T_c} + 2\left(\frac{S_k}{T_c}\right)^2\right)\right)^{-1}, \tag{3.38}$$

for all $\{\underline{U}, \underline{V}\}$. A similar analysis can be performed for the raised-cosine waveform, which has a pulse shape given by

$$\psi(t) = \sqrt{2/3}[1 - \cos(2\pi t/T_c)]p_{T_c}(t). \tag{3.39}$$

In [7], the autocorrelation functions for the raised-cosine waveform are shown to be

$$R_\psi(\tau) = \frac{2}{3}\tau + \frac{1}{3}\tau\cos\left(\frac{2\pi\tau}{T_c}\right) - \frac{T_c}{2\pi}\sin\left(\frac{2\pi\tau}{T_c}\right) \tag{3.40}$$

$$\hat{R}_\psi(\tau) = \frac{2}{3}(T_c - \tau) + \frac{1}{3}(T_c - \tau)\cos\left(\frac{2\pi\tau}{T_c}\right) + \frac{T_c}{2\pi}\sin\left(\frac{2\pi\tau}{T_c}\right). \tag{3.41}$$

The SINR is found following the same procedure as for the rectangular waveform, and

$$\Gamma(\underline{U}, \underline{V}) = \left(\frac{N_0}{E_s} + \sum_{k=1}^{K-1} \frac{A_k^2 P_k}{N A_0^2 P_0}\frac{1}{T_c^2}\left(\hat{R}_\psi^2(S_k) + R_\psi^2(S_k)\right)\right)^{-1} \tag{3.42}$$

for all $\{\underline{U}, \underline{V}\}$ where $R_\psi(S_k)$ and $\hat{R}_\psi(S_k)$ are as defined in equations (3.40) and (3.41) respectively. Note that $\Gamma(\underline{U}, \underline{V})$ does not depend on the phase offsets regardless of the chip waveform.

3.1.2 M-QAM with Fixed Delay Interference and Phase Offset Interference

From equations (3.29) and (3.30), it follows that

$$\begin{aligned}\mathrm{Var}(I_k^I|\mathcal{M}_k) + \mathrm{Var}(I_k^Q|\mathcal{M}_k) =& \frac{A_k^2 P_k}{2}\left[\gamma_k|u_{k,-1}|^2 + (N-\gamma_k)|u_{k,0}|^2\right]\hat{R}_{\psi_c}^2(S_k) \\ &+ \frac{A_k^2 P_k}{2}\left[(\gamma_k+1)|u_{k,-1}|^2 + (N-\gamma_k-1)|u_{k,0}|^2\right]R_{\psi_c}^2(S_k) \\ &+ \frac{A_k^2 P_k}{2}\left[\gamma_k|v_{k,-1}|^2 + (N-\gamma_k)|v_{k,0}|^2\right]\hat{R}_{\psi_c}^2(S_k) \\ &+ \frac{A_k^2 P_k}{2}\left[(\gamma_k+1)|v_{k,-1}|^2 + (N-\gamma_k-1)|v_{k,0}|^2\right]R_{\psi_c}^2(S_k). \end{aligned} \tag{3.43}$$

From equation (2.10), the average energy per channel symbol is given by

$$E_s = \mathrm{E}\left[|u_{0,0}|^2 + |v_{0,0}|^2\right]A_0^2 P_0 T = \frac{2(M-1)}{3}A_0^2 P_0 T, \tag{3.44}$$

and from equations (3.1) and (3.2).

$$\mathrm{E}\left[(S^I)^2\right] + \mathrm{E}\left[(S^Q)^2\right] = \frac{M-1}{3}A_0^2 P T^2 = \frac{E_s T}{2}. \tag{3.45}$$

Thus from equations (2.17) and (3.31), the SINR is given by

$$\Gamma(\underline{U}, \underline{V}) = \left(\frac{M-1}{3}\frac{N_0}{E_s} + \sum_{k=1}^{K-1}\frac{A_k^2 P_k}{A_0^2 P_0}\frac{1}{2T^2}\left(\mathrm{E}\left[(W_k^I)^2\middle|\,\mathcal{M}_k\right] + \mathrm{E}\left[(W_k^Q)^2\middle|\,\mathcal{M}_k\right]\right)\right)^{-1}. \tag{3.46}$$

Note, from equations (3.25) and (3.26), that equation (3.46) does not depend on the phase offsets of the interfering signals.

3.2 Symbol-Synchronous Interference

In this section, a system is considered in which each of the interfering signals is symbol synchronous with the desired signal at the receiver. (That is, $\tau_k = 0$, $1 \le k \le K-1$, and therefore

$S_k = 0$, $1 \leq k \leq K-1$.) Note that $\hat{R}_{\psi_c}(0) = T_c$ and $R_{\psi_c}(0) = 0$.

3.2.1 QPSK with Symbol-Synchronous Interference

From equation (3.37),

$$\mathrm{Var}(I_k^I|\mathcal{M}_k) = \mathrm{Var}(I_k^Q|\mathcal{M}_k) = \frac{A_k^2 P_k}{2} N T_c^2 \tag{3.47}$$

for all $\{\underline{U}, \underline{V}\}$. Therefore,

$$\Gamma(\underline{U}, \underline{V}) = \left(\frac{N_0}{E_s} + \sum_{k=1}^{K-1} \frac{A_k^2 P_k}{N A_0^2 P_0} \right)^{-1} \tag{3.48}$$

for all $\{\underline{U}, \underline{V}\}$.

3.2.2 M-QAM with Symbol-Synchronous Interference

From equations (3.29) and (3.30),

$$\mathrm{Var}\left(I_k^I|\mathcal{M}_k\right) = \frac{A_k^2 P_k}{2} \left[N|u_{k,0}|^2 T_c^2 \cos^2(\Phi_k) + N|v_{k,0}|^2 T_c^2 \sin^2(\Phi_k) \right] \tag{3.49}$$

and

$$\mathrm{Var}\left(I_k^Q|\mathcal{M}_k\right) = \frac{A_k^2 P_k}{2} \left[N|v_{k,0}|^2 T_c^2 \cos^2(\Phi_k) + N|u_{k,0}|^2 T_c^2 \sin^2(\Phi_k) \right]. \tag{3.50}$$

The SINR is thus given as

$$\Gamma(\underline{U}, \underline{V}) = \left(\frac{M-1}{3} \frac{N_0}{E_s} + \sum_{k=1}^{K-1} \left(|u_{k,0}|^2 + |v_{k,0}|^2 \right) \frac{A_k^2 P_k}{N A_0^2 P_0} \right)^{-1}. \tag{3.51}$$

for all $\{\underline{U}, \underline{V}\}$.

3.3 Uniformly Distributed Interference Delays

In this section, we consider interfering signals for which each delay, τ_k, is uniformly distributed over $[0, T)$ so that S_k is uniformly distributed over $[0, T_c)$ and γ_k is uniformly distributed over $\{0, 1, \ldots, N-1\}$.

3.3.1 QPSK with Uniform Interference Delays

Let

$$\Delta = \frac{1}{T_c}\int_0^{T_c} R_{\psi_c}^2(s)ds = \frac{1}{T_c}\int_0^{T_c} \hat{R}_{\psi_c}^2(s)ds. \tag{3.52}$$

for either waveform under consideration. From equations (3.29) and (3.30) for QPSK modulation

$$\begin{aligned}\mathrm{Var}\left(I_k^I|\mathcal{M}_k\right) &= \frac{A_k^2 P_k}{2}\left[2N\Delta\cos^2(\Phi_k) + 2N\Delta\sin^2(\Phi_k)\right] &(3.53)\\ &= A_k^2 P_k N\Delta &(3.54)\end{aligned}$$

and

$$\mathrm{Var}\left(I_k^Q|\mathcal{M}_k\right) = A_k^2 P_k N\Delta. \tag{3.55}$$

If the waveform is rectangular, $\Delta = \frac{1}{3}T_c^2$, so the SINR is given by

$$\Gamma(\underline{U},\underline{V}) = \left(\frac{N_0}{E_s} + \frac{2}{3N}\sum_{k=1}^{K-1}\frac{A_k^2 P_k}{A_0 P_0}\right)^{-1} \tag{3.56}$$

for each $\{\underline{U},\underline{V}\}$. If the strength of all received signals is the same, a result from [5] is obtained

$$\Gamma(\underline{U},\underline{V}) = \left(\frac{N_0}{E_s} + \frac{2(K-1)}{3N}\right)^{-1}. \tag{3.57}$$

For the raised-cosine chip waveform, the same technique as in [5] can be used with the autocorrelation function found in [7]. Using this method

$$\begin{aligned}\Delta = \frac{1}{T_c 576\,\pi^3}\Bigg(&320\,\cos\left(2\,\frac{\pi}{T_c}\right)\pi\,{T_c}^2 + 128\,\sin\left(2\,\frac{\pi}{T_c}\right)\pi^2 T_c - 160\,\sin\left(2\,\frac{\pi}{T_c}\right){T_c}^3 + \\ &8\,\sin\left(4\,\frac{\pi}{T_c}\right)\pi^2 T_c - 25\,\sin\left(4\,\frac{\pi}{T_c}\right){T_c}^3 + 28\,\cos\left(4\,\frac{\pi}{T_c}\right)\pi\,{T_c}^2 + 96\,\pi^3 + 72\,{T_c}^2\pi\Bigg)\\ = T_c^2\left(\frac{1}{6} + \frac{35}{48\pi^2}\right).\end{aligned} \tag{3.58}$$

Thus the SINR is given by

$$\Gamma(\underline{U},\underline{V}) = \left(\frac{1N_0}{2E_b} + \frac{2\left(\frac{1}{6}+\frac{35}{48\pi^2}\right)}{N}\sum_{k=1}^{K-1}\frac{A_k^2 P_k}{A_0^2 P_0}\right)^{-1}. \tag{3.59}$$

for all $\{\underline{U}, \underline{V}\}$.

3.3.2 M-QAM with Uniform Interference Delays

From equation (3.29), since

$$\mathrm{E}[\gamma_k] = \frac{N-1}{2}, \tag{3.60}$$

$$\begin{aligned}
\mathrm{Var}\left(I_k^I|\mathcal{M}_k\right) = {} & \frac{A_k^2 P_k}{2}\left[\left(\frac{N-1}{2}\right)|u_{k,-1}|^2 + \left(\frac{N+1}{2}\right)|u_{k,0}|^2\right]\Delta\cos^2(\Phi_k) \\
& + \frac{A_k^2 P_k}{2}\left[\left(\frac{N+1}{2}\right)|u_{k,-1}|^2 + \left(\frac{N-1}{2}\right)|u_{k,0}|^2\right]\Delta\cos^2(\Phi_k) \\
& + \frac{A_k^2 P_k}{2}\left[\left(\frac{N-1}{2}\right)|v_{k,-1}|^2 + \left(\frac{N+1}{2}\right)|v_{k,0}|^2\right]\Delta\sin^2(\Phi_k) \\
& + \frac{A_k^2 P_k}{2}\left[\left(\frac{N+1}{2}\right)|v_{k,-1}|^2 + \left(\frac{N-1}{2}\right)|v_{k,0}|^2\right]\Delta\sin^2(\Phi_k) \\
= {} & \frac{A_k^2 P_k}{2} N\Delta\left[|u_{k,-1}|^2 + |u_{k,0}|^2\right]\cos^2(\Phi_k) + \frac{A_k^2 P_k}{2} N\Delta\left[|v_{k,-1}|^2 + |v_{k,0}|^2\right]\sin^2(\Phi_k).
\end{aligned} \tag{3.61}$$

Similarly,

$$\mathrm{Var}\left(I_k^Q|\mathcal{M}_k\right) = \frac{A_k^2 P_k}{2} N\Delta\left[|v_{k,-1}|^2 + |v_{k,0}|^2\right]\cos^2(\Phi_k) + \frac{A_k^2 P_k}{2} N\Delta\left[|u_{k,-1}|^2 + |u_{k,0}|^2\right]\sin^2(\Phi_k). \tag{3.62}$$

The SINR is thus given by

$$\Gamma(\underline{U}, \underline{V}) = \left(\frac{M-1}{3}\frac{N_0}{E_s} + \sum_{k=1}^{K-1} N\Delta\left[|u_{k,-1}|^2 + |u_{k,0}|^2 + |v_{k,-1}|^2 + |v_{k,0}|^2\right]\frac{A_k^2 P_k}{2A_0^2 P_k T^2}\right)^{-1} \tag{3.63}$$

for all $\{\underline{U}, \underline{V}\}$. If the waveform is rectangular,

$$\Gamma(\underline{U}, \underline{V}) = \left(\frac{M-1}{3}\frac{N_0}{E_s} + \frac{1}{6}\sum_{k=1}^{K-1}\frac{A_k^2 P_k}{N A_0^2 P_k}\left[|u_{k,-1}|^2 + |u_{k,0}|^2 + |v_{k,-1}|^2 + |v_{k,0}|^2\right]\right)^{-1} \tag{3.64}$$

If the waveform is the raised-cosine function

$$\Gamma(\underline{U}, \underline{V}) = \left(\frac{M-1}{3}\frac{N_0}{E_s} + \frac{1}{2}\left(\frac{1}{6} + \frac{35}{48\pi^2}\right)\sum_{k=1}^{K-1}\frac{A_k^2 P_k}{N A_0^2 P_k}\left[|u_{k,-1}|^2 + |u_{k,0}|^2 + |v_{k,-1}|^2 + |v_{k,0}|^2\right]\right)^{-1}. \tag{3.65}$$

Chapter 4

Performance Evaluation and Approximation

In this chapter, we consider the probability of error of the system in Chapter 2. In particular, we compare the exact probability of error (obtained from Monte Carlo simulations using Matlab) with a Gaussian approximation to the probability of error. Given the channel symbols in the desired signal and the interfering signals, the Gaussian approximation replaces the decision statistics in equations (2.13) and (2.14) with independent Gaussian random with mean and variance determined by the mean and variance of the random variables they replace.

4.1 Closed-form expressions for the Gaussian Approximation

In this section, we obtain closed-form expressions for a Gaussian approximation to the probability of symbol error and the probability of bit error for the two modulations formats we use in the examples. Consider the condition that the channel symbol in the desired signal is $\{u_0, v_0\}$ and the channel symbols in the interfering signals are given by $\underline{U}$ and $\underline{V}$ in equations (2.15) and (2.16). One approach to the Gaussian approximation employs the approximations

$$\Pr(Z^I < w) \approx \mathrm{Q}\left(\frac{S^I - w}{\sigma_{N_I}}\right) \tag{4.1}$$

and

$$\Pr(Z^Q < y) \approx \mathrm{Q}\left(\frac{S^Q - y}{\sigma_{N_Q}}\right), \tag{4.2}$$

where

$$\mathrm{Q}(x) = \frac{1}{\sqrt{2\pi}} \int_x^\infty \exp\left(-\frac{u^2}{2}\right) du. \tag{4.3}$$

The expressions above account for a possible difference in the variance of N_I and the variance of N_Q. Instead, we employ a simplified Gaussian approximation in which we average the two variances for each approximation so that

$$\Pr(Z^I < w) \approx \mathrm{Q}\left(\sqrt{\frac{S^I - w}{\sigma}}\right) \tag{4.4}$$

and

$$\Pr(Z^Q < y) \approx \mathrm{Q}\left(\sqrt{\frac{S^Q - y}{\sigma}}\right), \tag{4.5}$$

where $\sigma^2 = \left(\sigma_{N_I}^2 + \sigma_{N_Q}^2\right)/2$. Using this approximation,

$$\Pr\left(Z^I < S^I - \sqrt{\frac{A_0^2 T^2 P_0}{8}}\right) = \Pr\left(Z^Q < S^Q - \sqrt{\frac{A_0^2 T^2 P_0}{8}}\right) = \mathrm{Q}\left(\sqrt{\Gamma(\underline{U}, \underline{V})}\right) \tag{4.6}$$

where $\Gamma(\underline{U}, \underline{V})$ is given by equation (2.17).

4.1.1 Closed-Form Approximations to the Probability of Error

The Gaussian approximation to the probability of error for QPSK modulation results in standard expressions for the probability of symbol error and the probability of bit error under Gray coding. Specifically,

$$P_s = 1 - \left(1 - \mathrm{Q}\left(\sqrt{\Gamma(\underline{U}, \underline{V})}\right)\right)^2 \tag{4.7}$$

and

$$P_b = \mathrm{Q}\left(\sqrt{\Gamma(\underline{U}, \underline{V})}\right). \tag{4.8}$$

The average probability of error is obtained by averaging over the distribution of $(\underline{U}, \underline{V})$.

The Gaussian approximation to the probability of error for M-QAM also results in standard expressions for the probability of symbol error and the probability of bit error under Gray coding. The probability of symbol error for an interior point in the signal constellation is

$$P_s = 4\,\mathrm{Q}(\sqrt{\Gamma(\underline{U},\underline{V})})\left(1 - \mathrm{Q}(\sqrt{\Gamma(\underline{U},\underline{V})})\right). \tag{4.9}$$

The probability of symbol error for a corner point in the signal constellation is

$$P_s = \mathrm{Q}(\sqrt{\Gamma(\underline{U},\underline{V})})\left(2 - \mathrm{Q}(\sqrt{\Gamma(\underline{U},\underline{V})})\right). \tag{4.10}$$

The probability of symbol error for a exterior point in the signal constellation that is not a corner point is

$$P_s = \mathrm{Q}(\sqrt{\Gamma(\underline{U},\underline{V})})\left(3 - 2\,\mathrm{Q}(\sqrt{\Gamma(\underline{U},\underline{V})})\right). \tag{4.11}$$

The probability of symbol error for each $\{\underline{U},\underline{V}\}$ is obtained by averaging these probabilities of error over the uniform distribution of the transmitted data symbols $\{u_{0,0}, v_{0,0}\}$. The resulting average probability of symbol error given $\{\underline{U},\underline{V}\}$ is given by

$$\begin{aligned} P_s = \frac{4}{M}\,\mathrm{Q}(\sqrt{\Gamma(\underline{U},\underline{V})})(2 - \mathrm{Q}(\sqrt{\Gamma(\underline{U},\underline{V})}) + \frac{(\sqrt{M}-2)4}{M}\,\mathrm{Q}(\sqrt{\Gamma(\underline{U},\underline{V})})(3 - 2\,\mathrm{Q}(\sqrt{\Gamma(\underline{U},\underline{V})})) \\ + \frac{4(M/4 - \sqrt{M}+1)}{M} 4\,\mathrm{Q}(\sqrt{\Gamma(\underline{U},\underline{V})})(1 - \mathrm{Q}(\sqrt{\Gamma(\underline{U},\underline{V})})). \end{aligned} \tag{4.12}$$

For 16-QAM, this simplifies to

$$P_s = 3\left(\mathrm{Q}\left(\sqrt{\Gamma(\underline{U},\underline{V})}\right) - \frac{1}{2}\,\mathrm{Q}^2\left(\sqrt{\Gamma(\underline{U},\underline{V})}\right)\right). \tag{4.13}$$

The relationship between the probability of symbol error and the probability of bit error for Gray-coded M-QAM depends on the value of M. The general form of the relationship is derived in [8]. For 16-QAM it is given by equation (9) of [8], which is expressed in our notation as .

$$P_b = \frac{3}{4}\,\mathrm{Q}(\sqrt{\Gamma(\underline{U},\underline{V})})(2 - \mathrm{Q}(\sqrt{\Gamma(\underline{U},\underline{V})}) + \frac{1}{2}\,\mathrm{Q}(\sqrt{9\Gamma(\underline{U},\underline{V})}) + \frac{1}{4}\,\mathrm{Q}(\sqrt{25\Gamma(\underline{U},\underline{V})}). \tag{4.14}$$

Since Gray coding is used, the bit mappings of nearest-neighbors in the signal constellation

differ by one bit. For sufficiently large values of $\Gamma(\underline{U}, \underline{V})$, the probability that more than one bit is in error in the detected data symbol is negligible. The probability of bit error for M=16 is thus approximated accurately by

$$P_b = \frac{3}{4} \mathrm{Q}(\sqrt{\Gamma(\underline{U}, \underline{V})}) \tag{4.15}$$

for values of the SINR of practical interest.

4.2 QPSK with Symbol Synchronous Inference

The performance of the system with QPSK modulation in the presence of symbol-synchronous interference is approximated using the Gaussian approximation and the results of Section 3.2.1 with equation (3.48). The accuracy of the approximation is shown in Figure 4.1, which illustrates the performance for a single symbol-synchronous interferer, no phase offset in the interferer, and various values of the spreading factor N. (The results do not depend on the chip waveform.) The accuracy of the approximation is considered for four values of the SIR: 0 dB, -3 dB, -6 dB, and -10 dB. Comparison of the simulation results with the Gaussian approximation shows that the approximation is quite accurate for large values of N, but there is a significant difference between the Gaussian approximation and the actual probability of error if N is small. As the signal-to-noise ratio E_b/N_0 increases, the probability of error approaches an error floor which is due to the interference. The error in the approximation is most noticeable as the performance approaches the error floor.

The performance predicted by the Gaussian approximation does not depend on the phase offset of the interfering signals, as shown in the previous chapter. The actual system performance *does* depend on the phase offset slightly, however, as shown in Figure 4.2 for various phase offsets, a spreading factor of eight, and equal-power received signals. (Once again, the results do not depend on the chip waveform.) The result of the Gaussian approximation is also shown, and once again it is seen that the accuracy of the approximation decreases as the signal-to-noise ratio is increased.

4.3 QPSK and Interference with a Fixed Delay

The performance of the system with QPSK modulation in the presence of interferers with arbitrary fixed delays is approximated using the Gaussian approximation and the results of Section 3.1.1. If the chip waveform of each transmission is rectangular, the value of $\Gamma(\underline{U}, \underline{V})$ used in the

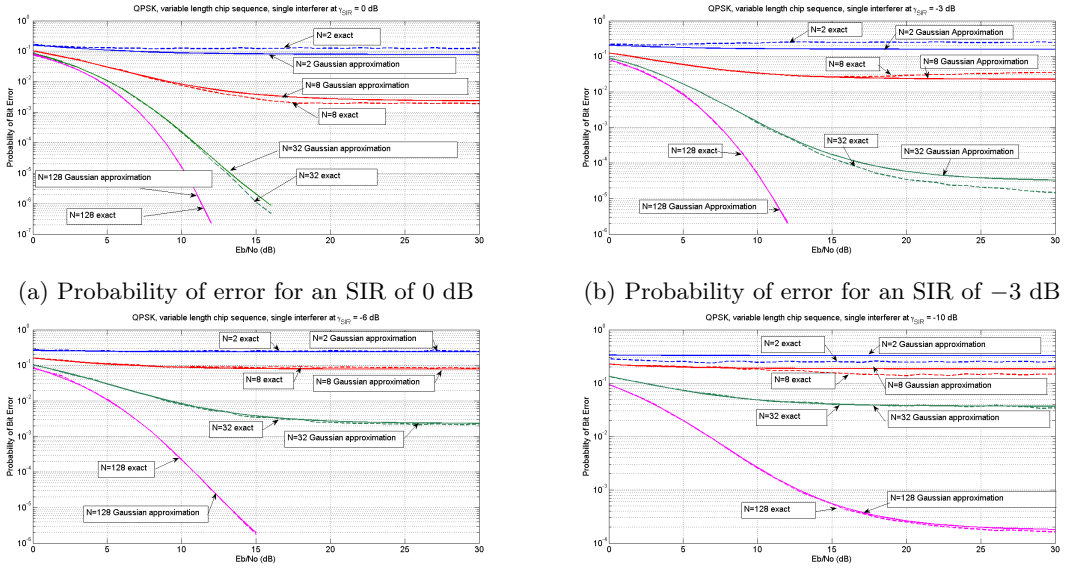

(a) Probability of error for an SIR of 0 dB

(b) Probability of error for an SIR of -3 dB

(c) Probability of error foran SIR of -6 dB

(d) Probability of error for an SIR of -10 dB

Figure 4.1: Probability of error for QPSK with two users and various values of N.

approximation is given by equation (3.38). Similarly, equation (3.42) is used if the chip waveform is the raised-cosine function. The accuracy of the approximation is shown in Figure 4.3, which illustrates the performance for a single interferer, a spreading factor of eight, equal-power received signals, and various values of the delay in the interferer. For either the waveform and any delay, the Gaussian approximation is accurate over the range of values of E_b/N_0 that are shown, though the accuracy decreases for larger values of E_b/N_0 (not shown in the figure).

4.4 QPSK with a Random Interference Delay

If a uniformly distributed random delay is imposed on each interfering signal, two different methods of Gaussian approximation can be employed. The first methods employs the variance of the interference after averaging over the random delay. The value of $\Gamma(\underline{U}, \underline{V})$ is given by equations (3.64) and (3.59) for rectangular and raised-cosine chip waveforms, respectively, with the average probability of bit error approximated by equation (4.14). The results of the approximation are shown for both waveforms in Figure 4.4a for a system with a single interferer, a spreading factor of eight, and equal-power received signals. The approximation is fairly accurate if the rectangular waveform is used, but it results in significant underestimation of the probability of error if the raised-cosine

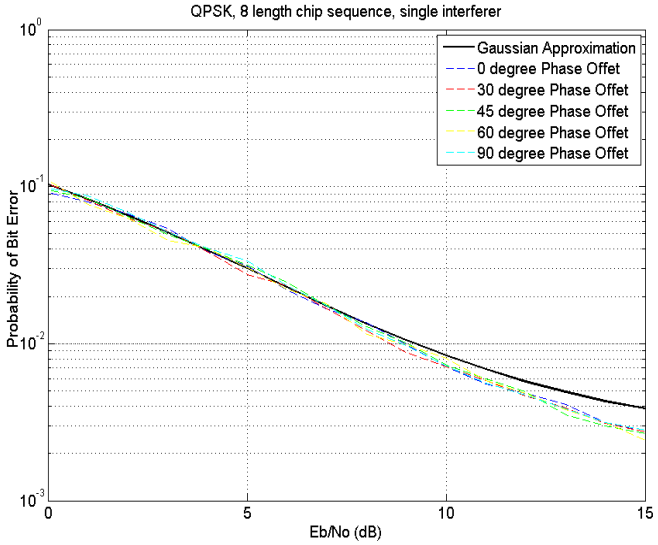

Figure 4.2: Probability of bit error for QPSK with various phases of interferer, $K = 2, N = 8$, and an SIR of 0 dB.

waveform is used, especially if the signal-to-noise ratio is large. The second method of Gaussian approximation first uses the approximation conditioned on the delay of each interferer. That is, it employs equation (4.14) together with equations (3.38) and (3.42) for the respective waveforms and each value of delay. The resulting approximations are given by

$$P_b = \int_0^1 \mathrm{Q}\left(\sqrt{\gamma_{SINR}(s)}\right) ds. \tag{4.16}$$

The accuracy of this approximation is shown in Figure 4.4b for the same system. The approximation using this method has similar accuracy to the first method if the rectangular waveform is used. It yields much greater accuracy than the first method if the raised-cosine waveform is used, however, especially if the signal-to-noise ratio is large.

4.5 M-QAM with Symbol Synchronous Inference

The performance of the system with M-QAM in the presence of symbol-synchronous interference is approximated using the Gaussian approximation and the results of Section 3.2.2 with equation (3.51). The accuracy of the approximation is shown in Figure 4.5 for 16-QAM, which illus-

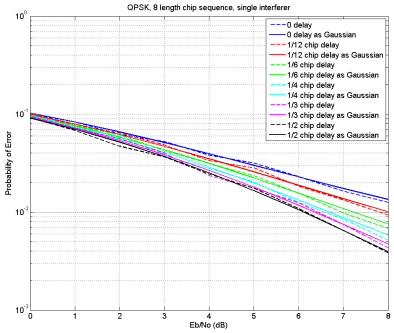

(a) Rectangular chip waveform.

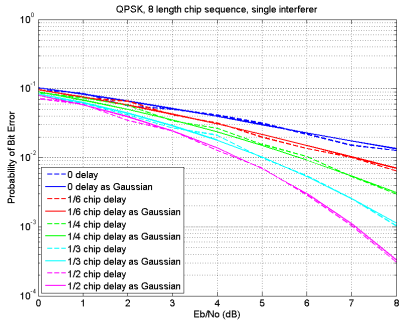

(b) Raised-cosine chip waveform.

Figure 4.3: Probability of bit error for QPSK with $K = 2$, various interference delays, $N = 8$, and an SIR of 0 dB.

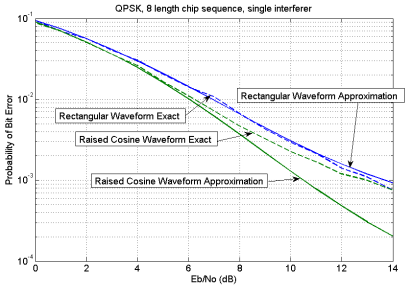

(a) First method of averaging over delay.

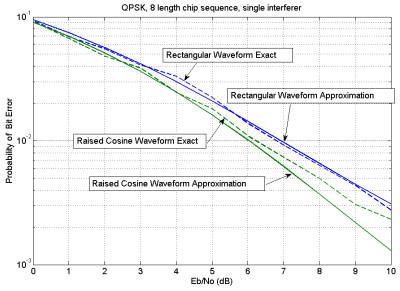

(b) Second method of averaging over delay.

Figure 4.4: Probability of bit error for QPSK with random interference delay, $K = 2$, $N = 8$, and an SIR of 0 dB.

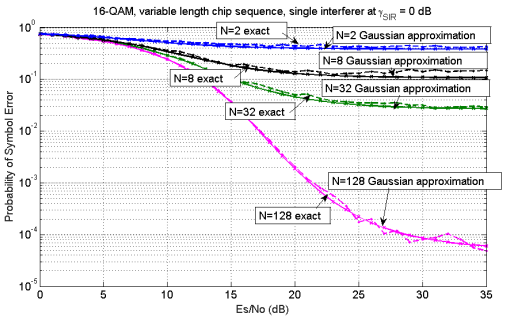

(a) Probability of error for $\gamma_{SIR} = 0$ dB

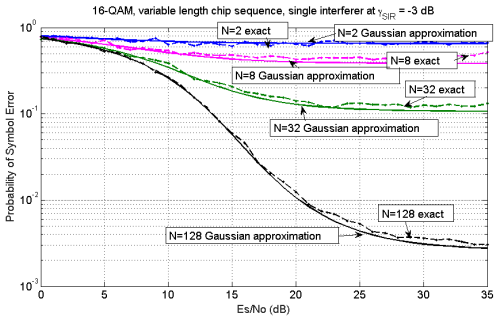

(b) Probability of error for $\gamma_{SIR} = -3$ dB

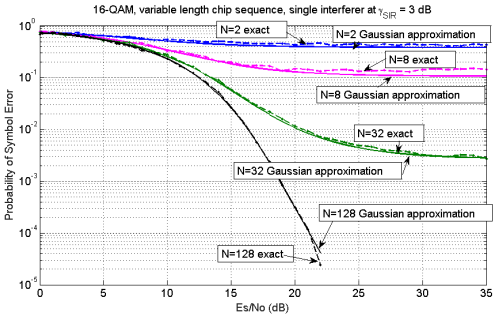

(c) Probability of error for $\gamma_{SIR} = 3$ dB

Figure 4.5: Probability of error for 16-QAM, chip and symbol synchronous, $K = 2$ and various values of N.

trates the performance for a single symbol-synchronous interferer, no phase offset in the interferer, and various values of the spreading factor N. (The results do not depend on the chip waveform.) The accuracy of the approximation is considered for four values of the SIR: -3 dB, 0 dB, and 3 dB. Comparison of the simulation results with the Gaussian approximation shows that the approximation is quite accurate for large values of N, with a moderate difference between the Gaussian approximation and the actual probability of error if N is small. As the signal-to-noise ratio E_b/N_0 increases, the probability of error approaches an error floor which is due to the interference. The error in the approximation is most noticeable as the performance approaches the error floor.

4.6 M-QAM and Interference with a Fixed Delay

The performance of the system with M-QAM in the presence of interferers with arbitrary fixed delays is approximated using the Gaussian approximation and the results of Section 3.1.2 with equation (4.13). If the chip waveform of each transmission is rectangular, the value of $\Gamma(\underline{U}, \underline{V})$ used in the approximation is given by equation (3.38). Similarly, equation (3.42) is used if the chip

waveform is the raised-cosine function. The accuracy of the approximation is shown in Figure 4.6, which illustrates the performance for 16-QAM, a single interferer, a spreading factor of 32, equal-power received signals, and various values of the delay in the interferer. Since each delay illustrated results in chip-synchronous interference, the results are the same for both waveforms. For each delay, the Gaussian approximation is accurate over the range of values of E_S/N_0 that are shown, though the accuracy decreases for larger values of E_S/N_0.

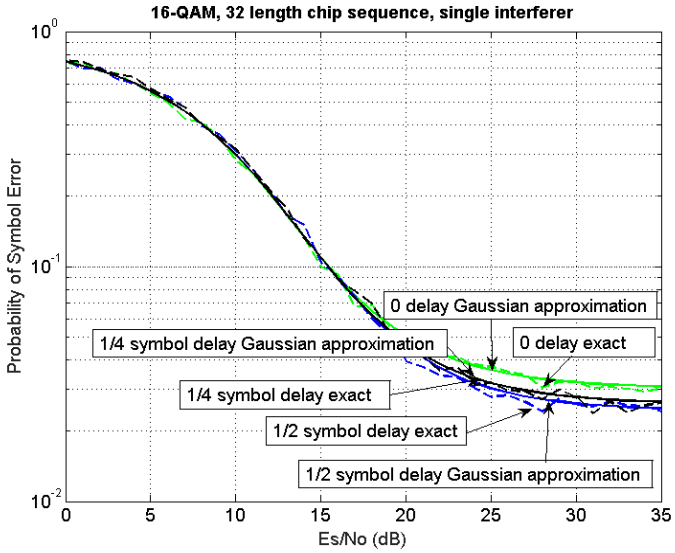

Figure 4.6: Probability of symbol error for 16-QAM with $K = 2$, various interference delays, and an SIR of 0 dB.

4.7 M-QAM with a Random Interference Delay

The second of the two methods of Gaussian approximation in Section 4.4 is considered in this section to approximate the probability of symbol error for the system using 16-QAM. The accuracy of the approximation is shown in Figure 4.7. The performance is shown for both the rectangular waveform and the raised-cosine waveform. The approximation using this method very high accuracy if the signal-to-noise ratio is small and reasonable accuracy if the signal-to-noise ratio is large.

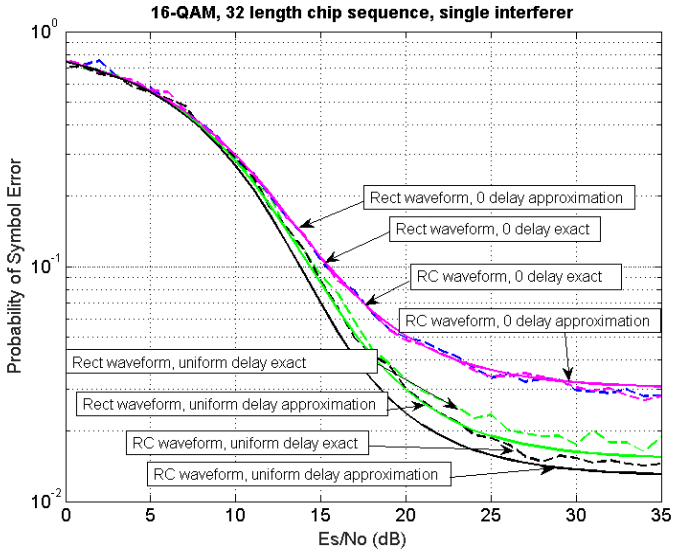

Figure 4.7: Probability of symbol error for 16-QAM with random interference delay, $K = 2$, $N = 32$, and an SIR of 0 dB.

Chapter 5

Conclusion

In this thesis, closed-form expressions are developed for the variance of the interference terms in the decision statistics of a DS-SS M-QAM communication system using coherent demodulation and matched-filter detection from a signal that is corrupted by multiple-access interference and thermal noise. The expressions are used in a Gaussian approximation to the probability of error at the receiver which results in a simple, closed-form expressions for the approximate probability of error. Two methods of Gaussian approximation are considered for the circumstance in which each interfering signal is subjected to a random delay relative to the desired signal. Examples of the approximations are examined for systems using QPSK modulation and 16-QAM is considered.

The accuracy of the approximations is very good for the system with QPSK modulation if the signal-to-noise ratio is small, but it is less accurate if the signal-to-noise ratio is large, especially in the presence of strong interference. Of the two methods of approximation under random delays, the method that averages over Gaussian approximations which are conditioned on the delays provides greater accuracy than the method that averages the interference variance over random delays prior to applying the Gaussian approximation. This difference is greater if the raised-cosine chip waveform is used than if the rectangular chop waveform is used. The approximations are accurate for the system with 16-QAM and fixed delays, and the second method of approximation under random delays is also accurate for the 16-QAM system.

Appendices

Appendix A Conditional Joint Distribution of Key Auxiliary Random Variables

In this appendix, we consider the conditional joint distribution of the $4(K-1)(N+1)$ random variables, $\mathcal{H}_{k,i} = \{H^I_{k,i}, \tilde{H}^I_{k,i}, H^Q_{k,i}, \tilde{H}^Q_{k,i}\}$, $0 \le i \le N$, $k = 1, \ldots, K-1$, defined in Chapter 3, given the magnitudes of the data symbols transmitted in the interval of interest. That is, conditioning is on the set of random variables $\mathcal{M} = \left\{\mathcal{M}_k = \{|u_{k,0}|, |u_{k,-1}|, |v_{k,0}|, |v_{k,-1}|\} \,|1 \le k \le K-1\right\}$. As in Chapter 3, the signature sequences of the desired signal are given.

Consider first the $(K-1)$ sets of random variables $\{\mathcal{H}_{k,i} | 0 \le i \le N\}$, for $k = 1, \le k \le K-1$. From the definitions of the random variables and the distributions specified in Section 2.5, it follows immediately that the $K-1$ sets are conditionally mutually independent given $\mathcal{M}$ and that conditioning for the kth set can be reduced to conditioning on $\mathcal{M}_k$.

The conditional mutual independence of the $(N+1)$ sets $\mathcal{H}_{k,i}$, $0 \le i \le N$, given $\mathcal{M}_k$ is established as follows. First condition on

$$\tilde{\mathcal{M}}_k = \{\mathrm{sgn}(|u_{k,0}|), \mathrm{sgn}(|u_{k,-1}|), \mathrm{sgn}(|v_{k,0}|), \mathrm{sgn}(|v_{k,-1}|)\}\,. \tag{A.1}$$

Each set $\mathcal{H}_{k,i}$ is a function of $\left\{a^I_{k,i-\gamma_k}, a^Q_{k,i-\gamma_k}\right\}$ for $1 \le i \le N-1$, and $\mathcal{H}_{k,N}$ is a function of $\left\{a^I_{k,i-\gamma_k-1}, a^Q_{k,i-\gamma_k-1}\right\}$. The sets $\left\{a^I_{k,i-\gamma_k}, a^Q_{k,i-\gamma_k}\right\}$, $0 \le i \le N$, are conditionally mutually independent given $\mathcal{M}_k$ and $\tilde{\mathcal{M}}_k$. The sets $\mathcal{H}_{k,i}$, $0 \le i \le N$, are thus conditionally mutually independent given $\mathcal{M}_k$ and $\tilde{\mathcal{M}}_k$.

The conditional joint distribution of $\mathcal{H}_{k,i}$ given $\mathcal{M}_k$ and $\tilde{\mathcal{M}}_k$ is uniform on the support

$$\begin{aligned}
\Big\{&(|u_{k,-1}|, |u_{k,-1}|, a^I_{0,i}a^Q_{0,i}|v_{k,-1}|, a^I_{0,i}a^Q_{0,i}|v_{k,-1}|),\\
&(|u_{k,-1}|, -|u_{k,-1}|, -a^I_{0,i}a^Q_{0,i}|v_{k,-1}|, a^I_{0,i}a^Q_{0,i}|v_{k,-1}|),\\
&(-|u_{k,-1}|, |u_{k,-1}|, a^I_{0,i}a^Q_{0,i}|v_{k,-1}|, -a^I_{0,i}a^Q_{0,i}|v_{k,-1}|),\\
&(-|u_{k,-1}|, -|u_{k,-1}|, -a^I_{0,i}a^Q_{0,i}|v_{k,-1}|, -a^I_{0,i}a^Q_{0,i}|v_{k,-1}|)\Big\}
\end{aligned}$$

given $\mathcal{M}_k$ and $\tilde{\mathcal{M}}_k$ for $0 \le i \le \gamma_{k-1}$. Similar results in terms of $|u_{k,0}|$ and $|u_{k,-1}|$ result for $\mathcal{H}_{k,i}, \gamma_k \le i \le N$.

In each case, the conditional joint distribution of $\mathcal{H}_{k,i}$ given $\mathcal{M}_k$ and $\tilde{\mathcal{M}}_k$ does not depend

on $\tilde{\mathcal{M}}_k$. The sets $\mathcal{H}_{k,i}$, $0 \leq i \leq N$, are thus conditionally mutually independent given $\mathcal{M}_k$. Each random variable in $\mathcal{H}_{k,i}$ has a conditional mean of zero given $\mathcal{M}_k$,

$$\mathrm{E}\left[\left(H_{k,i}^{I}\right)^{2}|\mathcal{M}_k\right] = \mathrm{E}\left[\left(\tilde{H}_{k,i}^{I}\right)|\mathcal{M}_k\right] = \begin{cases} |u_{k,-1}|^2, 0 \leq i \leq \gamma_k - 1 \\ |u_{k,0}|^2, \gamma_k \leq i \leq N-1 \\ |u_{k,-1}|^2, i = N \end{cases} \tag{A.2}$$

$$\mathrm{E}\left[\left(H_{k,i}^{Q}\right)^{2}|\mathcal{M}_k\right] = \mathrm{E}\left[\left(\tilde{H}_{k,i}^{Q}\right)|\mathcal{M}_k\right] = \begin{cases} |v_{k,-1}|^2, 0 \leq i \leq \gamma_k - 1 \\ |v_{k,0}|^2, \gamma_k \leq i \leq N-1 \\ |v_{k,-1}|^2, i = N. \end{cases} \tag{A.3}$$

The four random variables $\mathcal{H}_{k,i} = \{H_{k,i}^{I}, \tilde{H}_{k,i}^{I}, H_{k,i}^{Q}, \tilde{H}_{k,i}^{Q}\}$ are *not* conditionally mutually independent given $\mathcal{M}_k$ for $0 \leq i \leq N$. This is seen by noting that the fourth moment

$$\mathrm{E}\left[H_{k,i}^{I}\cdots\tilde{H}_{k,i}^{Q}|\mathcal{M}_k\right] = \begin{cases} |u_{k,-1}|^2|v_{k,-1}|^2 \neq 0, 0 \leq i \leq \gamma_k - 1, i = N \\ |u_{k,0}|^2|v_{k,0}|^2 \neq 0, \gamma_k \leq N-1 \end{cases} \tag{A.4}$$

whereas, each of the four has a conditional mean of zero given $\mathcal{M}_k$. From the conditional distributions noted above, $H_{k,i}^{I}$ and $\tilde{H}_{k,i}^{I}$ are conditionally independent given $\mathcal{M}_k$, as are each pair of random variables, $\left\{H_{k,i}^{I}H_{k,i}^{Q}\right\}$, $\left\{\tilde{H}_{k,i}^{I}\tilde{H}_{k,i}^{Q}\right\}$, and $\left\{H_{k,i}^{Q}\tilde{H}_{k,i}^{Q}\right\}$, for $0 \leq i \leq N$. The remaining pairs of random variables in H_k, i are conditionally correlated given $\mathcal{M}_k$, however. For example,

$$\mathrm{E}\left[H_{k,i}^{I}\tilde{H}_{k,i}^{Q}|\mathcal{M}_k\right] = \begin{cases} |u_{k,-1}||v_{k,-1}|a_{0,i}^{I}, a_{0,i}^{Q}, 0 \leq i \leq \gamma_k - 1, \\ |u_{k,0}||v_{k,0}|a_{0,i}^{I}, a_{0,i}^{Q}, \neq 0, \\ |u_{k,-1}|^2|v_{k,-1}|a_{0,0}^{I}a_{0,0}^{Q}, i = N, \end{cases} \tag{A.5}$$

(Recall that $a_{0,i}^{I}$ and $a_{0,i}^{Q}$ are given for each i.) The same result follows for $\mathrm{E}\left[\tilde{H}_{k,i}^{I}H_{k,i}^{Q}|\mathcal{M}_k\right]$. Note that the conditional correlation coefficient of the pair of random variables given $\mathcal{M}_k$ has a magnitude of one in either case.

Appendix B Characterization of Multiple-Access Interference

In this appendix, we consider the multiple-access interference terms in equations (2.13) and (2.14) by considering the random variables $\left\{U_k^I, V_k^I, U_k^Q, V_k^Q\right\}$, $1, \leq k, \leq K-1$, defined in equations (3.6), (3.7), (3.10) and (3.11). As in Appendix A, conditioning is on $\mathcal{M}$, and the signature sequences of the desired signal are given. The development in this appendix is patterned after the analogous development in [5] for a system with OQPSK DS-SS modulation.

Following [5], we can show that

$$U_k^I = \lambda_k^I \hat{R}_{\psi_c}(S_k) + \mu_k^I R_{\psi_c}(S_k) \tag{B.6}$$

where

$$\lambda_k^I = X_k^I + Y_k^I + H_{k,N-1}^I \tag{B.7}$$

and

$$\mu_k^I = X_k^I - Y_k^I + H_{k,N}^I \tag{B.8}$$

The random variables X_k^I and Y_k^I are given by

$$X_k^I = \sum_{i \in \mathcal{A}^I} H_{k,i}^I \tag{B.9}$$

and

$$Y_k^I = \sum_{i \in \mathcal{B}^I} H_{k,i}^I \tag{B.10}$$

where

$$\mathcal{A}^I = \left\{i, 0 \leq i \leq N-2 | a_{0,i}^I a_{0,i+1}^I = +1\right\} \tag{B.11}$$

and

$$\mathcal{B}^I = \left\{i, 0 \leq i \leq N-2 | a_{0,i}^I a_{0,i+1}^I = -1\right\}. \tag{B.12}$$

In a similar manner,

$$V_k^I = \tilde{\lambda}_k^I \hat{R}_{\psi_c}(S_k) + \tilde{\mu}_k^I R_{\psi_c}(S_k) \tag{B.13}$$

where

$$\tilde{\lambda}_k^I = \tilde{X}_k^I + \tilde{Y}_k^I + \tilde{H}_{k,N-1}^I \tag{B.14}$$

and

$$\tilde{\mu}_k^I = \tilde{X}_k^I - \tilde{Y}_k^I + \tilde{H}_{k,N}^I. \tag{B.15}$$

The random variables $\tilde{X}_k^I$ and $\tilde{Y}_k^I$ are given by

$$\tilde{X}_k^I = \sum_{i \in \mathcal{A}^I} \tilde{H}_{k,i}^I \tag{B.16}$$

and

$$\tilde{Y}_k^I = \sum_{i \in \mathcal{B}^I} \tilde{H}_{k,i}^I. \tag{B.17}$$

Furthermore,

$$U_k^Q = \lambda_k^Q \hat{R}_{\psi_c}(S_k) + \mu_k^Q R_{\psi_c}(S_k) \tag{B.18}$$

where

$$\lambda_k^Q = X_k^Q + Y_k^Q + H_{k,N-1}^Q \tag{B.19}$$

and

$$\mu_k^Q = X_k^Q - Y_k^Q + H_{k,N}^Q \tag{B.20}$$

The random variables X_k^Q and Y_k^Q are given by

$$X_k^Q = \sum_{i \in \mathcal{A}^Q} H_{k,i}^Q \tag{B.21}$$

and

$$Y_k^Q = \sum_{i \in \mathcal{B}^Q} H_{k,i}^Q \tag{B.22}$$

where $\mathcal{A}^Q$ and $\mathcal{B}^Q$ are define as

$$\mathcal{A}^Q = \left\{ i, 0 \leq i \leq N-2 | a_{0,i}^Q a_{0,i+1}^Q = +1 \right\} \tag{B.23}$$

and

$$\mathcal{B}^Q = \left\{ i, 0 \leq i \leq N-2 | a_{0,i}^Q a_{0,i+1}^Q = -1 \right\}. \tag{B.24}$$

Similarly,

$$V_k^Q = \tilde{\lambda}_k^Q \hat{R}_{\psi_c}(S_k) + \tilde{\mu}_k^Q R_{\psi_c}(S_k) \tag{B.25}$$

where

$$\tilde{\lambda}_k^Q = \tilde{X}_k^Q + \tilde{Y}_k^Q + \tilde{H}_{k,N-1}^Q \tag{B.26}$$

and

$$\tilde{\mu}_k^Q = \tilde{X}_k^Q - \tilde{Y}_k^I + \tilde{H}_{k,N}^Q. \tag{B.27}$$

The random variables $\tilde{X}_k^Q$ and $\tilde{Y}_k^Q$ are given by

$$\tilde{X}_k^Q = \sum_{i \in \mathcal{A}^Q} \tilde{H}_{k,i}^Q \tag{B.28}$$

and

$$\tilde{Y}_k^Q = \sum_{i \in \mathcal{B}^Q} \tilde{H}_{k,i}^Q. \tag{B.29}$$

Since the signature sequences of the desired signal are given, so are $\mathcal{A}^I$, $\mathcal{B}^I$, $\mathcal{A}^Q$, and $\mathcal{B}^Q$. Consequently, the $(K-1)$ sets

$$\Big\{X_k^I, Y_k^I, \tilde{X}_k^I, \tilde{Y}_k^I, X_k^Q, Y_k^Q, \tilde{X}_k^Q, \tilde{Y}_k^Q, H_{k,N-1}^I, H_{k,N}^I, \tilde{H}_{k,N-1}^I, \tilde{H}_{k,N}^I, H_{k,N-1}^Q, H_{k,N}^Q, \tilde{H}_{k,N-1}^Q, \tilde{H}_{k,N}^Q, \Big\},$$

$1 \le k \le K-1$ are conditionally mutually independent given $\mathcal{M}$, from the results of Appendix A. Consequently, so are the $(K-1)$ sets $\left\{U_k^I, V_k^I, U_k^Q, V_k^Q\right\}$, $1 \le k \le K-1$. Furthermore, for each k, the conditioning can be reduced to conditioning on $\mathcal{M}_k$.

Equations (B.6), (B.13), (B.18), and (B.25) can be expanded as

$$U_k^I = X_k^I f(S_k) + Y_k^I g(S_k) + H_{k,N-1}^I \hat{R}_{\psi_c}(S_k) + H_{k,N}^I R_{\psi_c}(S_k), \tag{B.30}$$

$$V_k^I = \tilde{X}_k^I f(S_k) + \tilde{Y}_k^I g(S_k) + \tilde{H}_{k,N-1}^I \hat{R}_{\psi_c}(S_k) + \tilde{H}_{k,N}^I R_{\psi_c}(S_k), \tag{B.31}$$

$$U_k^Q = X_k^Q f(S_k) + Y_k^Q g(S_k) + H_{k,N-1}^Q \hat{R}_{\psi_c}(S_k) + H_{k,N}^Q R_{\psi_c}(S_k), \tag{B.32}$$

and

$$V_k^Q = \tilde{X}_k^Q f(S_k) + \tilde{Y}_k^Q g(S_k) + \tilde{H}_{k,N-1}^Q \hat{R}_{\psi_c}(S_k) + \tilde{H}_{k,N}^Q R_{\psi_c}(S_k). \tag{B.33}$$

where

$$f(s) = \hat{R}_{\psi_c}(s) + R_{\psi_c}(s) \tag{B.34}$$

and

$$g(s) = \hat{R}_{\psi_c}(s) - R_{\psi_c}(s). \tag{B.35}$$

The subsets $\mathcal{A}^I$, $\mathcal{B}^I$, $\{N-1\}$, and $\{N\}$ are disjoint, as are the subsets $\mathcal{A}^Q$, $\mathcal{B}^Q$, $\{N-1\}$, and $\{N\}$. Thus each of the four sets $\left\{X_k^I, X_k^I, H_{k,N-1}^I, H_{k,N}^I\right\}$, $\left\{\tilde{X}_k^I, \tilde{Y}_k^I, \tilde{H}_{k,N-1}^I, \tilde{H}_{k,N}^I\right\}$, $\left\{X_k^Q, Y_k^Q, H_{k,N-1}^Q, H_{k,N}^Q\right\}$, and $\left\{\tilde{X}_k^Q, \tilde{Y}_k^Q, \tilde{H}_{k,N-1}^Q, \tilde{H}_{k,N}^Q\right\}$ is a set of conditionally independent random variables given $\mathcal{M}_k$. From the results of Appendix A, however, there are dependencies across the four sets.

The dependence on the signature sequences of the desired signal can be expressed in a simple manner as follows. As shown in [4],

$$\left|\mathcal{A}^I\right| = \frac{N-1+C^I}{2} \tag{B.36}$$

and

$$\left|\mathcal{B}^I\right| = \frac{N-1-C^I}{2} \tag{B.37}$$

where

$$C^I = \sum_{j=0}^{N-2} a_{0,j}^I a_{0,j+1}^I \tag{B.38}$$

is the single-offset *aperiodic autocorrelation* [6] of the inphase signature sequence of the desired signal.

Similarly

$$\left|\mathcal{A}^Q\right| = \frac{N-1+C^Q}{2} \tag{B.39}$$

and

$$\left|\mathcal{B}^Q\right| = \frac{N-1-C^Q}{2} \tag{B.40}$$

where

$$C^Q = \sum_{j=0}^{N-2} a_{0,j}^Q a_{0,j+1}^Q \tag{B.41}$$

is the single-offset aperiodic autocorrelation of the quadrature signature sequence of the desired

signal.

From equations (B.9),(B.10),(B.16),(B.17),(B.21),(B.22),(B.28), and (B.29), the conditional joint distribution of

$$\left\{X_k^I, Y_k^I, \tilde{X}_k^I, \tilde{Y}_k^I, X_k^Q, Y_k^Q, \tilde{X}_k^Q, \tilde{Y}_k^Q\right\}$$

given $\mathcal{M}_k$ depends on the signature sequences of the desired signal only through C^I and C^Q. The same result follows for the conditional joint distribution of $\left\{U_k^I, V_k^I, U_k^Q, V_k^Q\right\}$ given $\mathcal{M}_k$.

From the definitions of λ_k^I, μ_k^I, $\tilde{\lambda}_k^I$, $\tilde{\mu}_k^I$, λ_k^Q, μ_k^Q, $\tilde{\lambda}_k^Q$, and $\tilde{\mu}_k^Q$, it follows that each has a conditional mean of zero given $\mathcal{M}_k$ for $1 \leq k \leq K-1$. The conditional second moments given $\mathcal{M}_k$ are determined as follows. We can express X_k^I and Y_k^I as

$$X_k^I = \sum_{i \in \mathcal{A}_1^I} H_{k,i}^I + \sum_{i \in \mathcal{A}_2^I} H_{k,i}^I \tag{B.42}$$

and

$$Y_k^I = \sum_{i \in \mathcal{B}_1^I} H_{k,i}^I + \sum_{i \in \mathcal{B}_2^I} H_{k,i}^I \tag{B.43}$$

where

$$\mathcal{A}_1^I = A^I \cap \{i | 0 \leq i \leq \gamma_{k-1}\} \tag{B.44}$$

$$\mathcal{A}_2^I = A^I \cap \{i | \gamma_{k-1} \leq i \leq N-2\} \tag{B.45}$$

and $\mathcal{B}_1^I$ and $\mathcal{B}_1^I$ are defined similarly. The random variables $\tilde{X}_k^I$ and $\tilde{Y}_k^I$ can be expressed similarly in terms of $\mathcal{A}_1^I$, $\mathcal{A}_2^I$, $\mathcal{B}_1^I$, and $\mathcal{B}_2^I$. And the random variables X_k^Q, X_k^Q, $\tilde{X}_k^Q$ and $\tilde{Y}_k^Q$ can be expressed similarly in terms of analogous sets $\mathcal{A}_1^Q$, $\mathcal{A}_2^Q$, $\mathcal{B}_1^Q$, and $\mathcal{B}_2^Q$.

Then

$$\begin{aligned}
\mathrm{E}\left[\left(\lambda_k^I\right)^2|\mathcal{M}_k\right] &= \mathrm{E}\left[\left(\sum_{i\in\mathcal{A}_1^I} H_{k,i}^I + \sum_{i\in\mathcal{A}_2^I} H_{k,i}^I + \sum_{i\in\mathcal{B}_1^I} H_{k,i}^I + \sum_{i\in\mathcal{B}_2^I} H_{k,i}^I + H_{k,N-1}^I\right)^2|\mathcal{M}_k\right] \\
&= \sum_{i\in\mathcal{A}_1^I}\mathrm{E}\left[\left(H_{k,i}^I\right)^2|\mathcal{M}_k\right] + \sum_{i\in\mathcal{A}_2^I}\mathrm{E}\left[\left(H_{k,i}^I\right)^2|\mathcal{M}_k\right] + \sum_{i\in\mathcal{B}_1^I}\mathrm{E}\left[\left(H_{k,i}^I\right)^2|\mathcal{M}_k\right] \\
&\qquad + \sum_{i\in\mathcal{B}_2^I}\mathrm{E}\left[\left(H_{k,i}^I\right)^2|\mathcal{M}_k\right] + \mathrm{E}\left[\left(H_{k,N-1}^I\right)^2|\mathcal{M}_k\right] \\
&= \gamma_k\left|u_{k,-1}\right|^2 + (N-1-\gamma_k)\left|u_{k,0}\right|^2 + \left|u_{k,0}\right|^2 \\
&= \gamma_k\left|u_{k,-1}\right|^2 + (N-\gamma_k)\left|u_{k,0}\right|^2
\end{aligned} \tag{B.46}$$

since $\left|\mathcal{A}_1^I\right| + \left|\mathcal{B}_1^I\right| = \gamma_k$ and $\left|\mathcal{A}_2^I\right| + \left|\mathcal{B}_2^I\right| = N-1-\gamma_k$. Similarly,

$$\mathrm{E}\left[\left(\tilde{\lambda}_k^I\right)^2|\mathcal{M}_k\right] = \gamma_k\left|u_{k,-1}\right|^2 + (N-\gamma_k)\left|u_{k,0}\right|^2, \tag{B.47}$$

$$\mathrm{E}\left[\left(\mu_k^I\right)^2|\mathcal{M}_k\right] = (\gamma_k+1)\left|u_{k,-1}\right|^2 + (N-\gamma_k-1)\left|u_{k,0}\right|^2, \tag{B.48}$$

and

$$\mathrm{E}\left[\left(\tilde{\mu}_k^I\right)^2|\mathcal{M}_k\right] = (\gamma_k+1)\left|u_{k,-1}\right|^2 + (N-\gamma_k-1)\left|u_{k,0}\right|^2. \tag{B.49}$$

Similar steps result in

$$\begin{aligned}
\mathrm{E}\left[\left(\lambda_k^Q\right)^2|\mathcal{M}_k\right] &= \mathrm{E}\left[\left(\tilde{\lambda}_k^Q\right)^2|\mathcal{M}_k\right] \\
&= \gamma_k\left|v_{k,-1}\right|^2 + (N-\gamma_k)\left|v_{k,0}\right|^2
\end{aligned} \tag{B.50}$$

and

$$\begin{aligned}
\mathrm{E}\left[\left(\mu_k^Q\right)^2|\mathcal{M}_k\right] &= \mathrm{E}\left[\left(\tilde{\mu}_k^Q\right)^2|\mathcal{M}_k\right] \\
&= (\gamma_k+1)\left|v_{k,-1}\right|^2 + (N-\gamma_k-1)\left|v_{k,0}\right|^2
\end{aligned} \tag{B.51}$$

From the results of Appendix A, for each pair of the random variables the conditional crosscorrelation given $\mathcal{M}_k$ is zero, except in the following instances.

From the definitions of the random variables,

$$\begin{aligned}\mathrm{E}\left[\lambda_k^I \mu_k^I | \mathcal{M}_k\right] &= \sum_{i\in\mathcal{A}_1^I} |u_{k,-1}|^2 + \sum_{i\in\mathcal{A}_2^I} |u_{k,0}|^2 - \sum_{i\in\mathcal{B}_1^I} |u_{k,-1}|^2 - \sum_{i\in\mathcal{B}_2^I} |u_{k,0}|^2 \\ &= \left(\left|\mathcal{A}_1^I\right| - \left|\mathcal{B}_1^I\right|\right) |u_{k,-1}|^2 + \left(\left|\mathcal{A}_2^I\right| - \left|\mathcal{B}_2^I\right|\right) |u_{k,0}|^2 ,\end{aligned} \tag{B.52}$$

$$E\left[\tilde{\lambda}_k^I \tilde{\mu}_k^I | \mathcal{M}_k\right] = \left(\left|\mathcal{A}_1^I\right| - \left|\mathcal{B}_1^I\right|\right) |u_{k,-1}|^2 + \left(\left|\mathcal{A}_2^I\right| - \left|\mathcal{B}_2^I\right|\right) |u_{k,0}|^2 , \tag{B.53}$$

and

$$E\left[\lambda_k^Q \mu_k^Q | \mathcal{M}_k\right] = E\left[\tilde{\lambda}_k^Q \tilde{\mu}_k^Q | \mathcal{M}_k\right] = \left(\left|\mathcal{A}_1^I\right| - \left|\mathcal{B}_1^I\right|\right) |v_{k,-1}|^2 + \left(\left|\mathcal{A}_2^I\right| - \left|\mathcal{B}_2^I\right|\right) |v_{k,0}|^2 . \tag{B.54}$$

In a similar manner,

$$\begin{aligned}E\left[\lambda_k^I \tilde{\lambda}_k^Q | \mathcal{M}_k\right] &= E\left[\tilde{\lambda}_k^I \lambda_k^Q | \mathcal{M}_k\right] \\ &= |u_{k,-1}|\,|v_{k,-1}| \left(\sum_{i=0}^{\gamma_{k-1}} a_{0,i}^I a_{0,i}^Q\right) + |u_{k,0}|\,|v_{k,0}| \left(\sum_{i=\gamma_{k-1}}^{N-2} a_{0,i}^I a_{0,i}^Q\right),\end{aligned} \tag{B.55}$$

$$\begin{aligned}E\left[\lambda_k^I \tilde{\mu}_k^Q | \mathcal{M}_k\right] = E\left[\mu_k^I \tilde{\lambda}_k^Q | \mathcal{M}_k\right] = E\left[\tilde{\lambda}_k^I \mu_k^Q | \mathcal{M}_k\right] = E\left[\tilde{\mu}_k^I \lambda_k^Q | \mathcal{M}_k\right] \\ = |u_{k,-1}|\,|v_{k,-1}| \left(\sum_{i=0}^{\gamma_{k-1}} a_{0,i}^I a_{0,i}^Q\right) - |u_{k,0}|\,|v_{k,0}| \left(\sum_{i=\gamma_k}^{N-2} a_{0,i}^I a_{0,i}^Q\right),\end{aligned} \tag{B.56}$$

and

$$\begin{aligned}E\left[\mu_k^I \tilde{\mu}_k^Q | \mathcal{M}_k\right] &= E\left[\tilde{\mu}_k^I \mu_k^Q | \mathcal{M}_k\right] \\ &= |u_{k,-1}|\,|v_{k,-1}|\, a_{0,0}^I a_{0,0}^Q + |u_{k,-1}|\,|v_{k,-1}| \left(\sum_{i=0}^{\gamma_{k-1}} a_{0,i}^I a_{0,i}^Q\right) \\ &\quad + |u_{k,0}|\,|v_{k,0}| \left(\sum_{i=\gamma_k}^{N-2} a_{0,i}^I a_{0,i}^Q\right).\end{aligned} \tag{B.57}$$

The remaining conditional second moments of the random variables are defined by equations (B.7), (B.8), (B.14), (B.15), (B.19), (B.20), (B.26), and (B.27), and are all zero. The conditional first and second moments of $\left\{U_k^I, V_k^I, U_k^Q, V_k^Q\right\}$ given $\mathcal{M}_k$ follow from equations (B.6), (B.13), (B.18), (B.25)

and equations (B.46) - (B.57). In particular, the conditional mean of each given $\mathcal{M}_k$ is zero.

Appendix C Moments of Interference Terms With Random Signature Sequences

In this appendix, we consider the first and second conditional moments of the multiple-access interference terms $\left\{W_k^I, W_k^Q\right\}$, $1 \leq k \leq K-1$, given $\mathcal{M}$. Unlike the previous appendices, we consider the expected value of the moments with respect to uniformly distributed signature sequences for the desired signal. From the results of Appendix B it follows that the $(K-1)$ sets $\left\{U_k^I, V_k^I, U_k^Q, V_k^Q\right\}$, $1 \leq k \leq K-1$, are conditionally uncorrelated given $\mathcal{M}$ under expectation with respect to the signature sequences of the desired signal, and conditioning for the kth set can be reduced to $\mathcal{M}_k$.

Under this expectation, the expressions for several quantities considered in Appendix B are simplified. In particular, from equations (B.52) - (B.54),

$$\mathrm{E}\left[\lambda_k^I \mu_k^I | \mathcal{M}_k\right] = \mathrm{E}\left[\tilde{\lambda}_k^I \tilde{\mu}_k^I | \mathcal{M}_k\right] = \mathrm{E}\left[\lambda_k^Q \mu_k^Q | \mathcal{M}_k\right] = \mathrm{E}\left[\tilde{\lambda}_k^Q \tilde{\mu}_k^Q | \mathcal{M}_k\right] = 0, \tag{C.58}$$

since

$$\mathrm{E}\left[|A_1^I|\right] = \mathrm{E}\left[|B_1^I|\right] = \frac{\gamma_k}{2}, \tag{C.59}$$

$$\mathrm{E}\left[|A_2^I|\right] = \mathrm{E}\left[|B_2^I|\right] = \frac{N-1-\gamma_k}{2}, \tag{C.60}$$

$$\mathrm{E}\left[|A_1^Q|\right] = \mathrm{E}\left[|B_1^Q|\right] = \frac{\gamma_k}{2}, \tag{C.61}$$

and

$$\mathrm{E}\left[|A_2^Q|\right] = \mathrm{E}\left[|B_2^Q|\right] = \frac{N-1-\gamma_k}{2}, \tag{C.62}$$

Similarly, from equations (B.55) - (B.57),

$$\mathrm{E}\left[\lambda_k^I \tilde{\lambda}_k^Q | \mathcal{M}_k\right] = \mathrm{E}\left[\tilde{\lambda}_k^I \lambda_k^Q | \mathcal{M}_k\right] = \mathrm{E}\left[\mu_k^I \tilde{\mu}_k^Q | \mathcal{M}_k\right] = \mathrm{E}\left[\tilde{\mu}_k^I \mu^Q | \mathcal{M}_k\right] = 0 \tag{C.63}$$

and

$$\mathrm{E}\left[\lambda_k^I \tilde{\mu}_k^Q | \mathcal{M}_k\right] = \mathrm{E}\left[\mu_k^I \lambda_k^Q | \mathcal{M}_k\right] = \mathrm{E}\left[\tilde{\lambda}_k^I \mu_k^Q | \mathcal{M}_k\right] = \mathrm{E}\left[\tilde{\mu}_k^I \lambda^Q | \mathcal{M}_k\right] = 0 \tag{C.64}$$

The remaining conditional second moments of the random variables defined by equations (B.7), (B.8),(B.14),(B.15),(B.19),(B.20),(B.26), and (B.27) are all zero. From equations (B.6)-(B.25), under expectation with respect to uniform signature sequences,

$$\mathrm{E}[U_k^I | \tilde{\mathcal{M}}_k] = \mathrm{E}[V_k^I | \tilde{\mathcal{M}}_k] = \mathrm{E}[U_k^Q | \tilde{\mathcal{M}}_k] = \mathrm{E}[V_k^I | \tilde{\mathcal{M}}_k] = 0, \tag{C.65}$$

$$\begin{aligned} \mathrm{E}\left[(U_k^I)^2 | \tilde{\mathcal{M}}_k\right] &= \mathrm{E}\left[(\lambda_k^I)^2 | \tilde{\mathcal{M}}_k\right] \hat{R}_{\psi_c}^2(S_k) + \mathrm{E}\left[(\mu_k^I)^2 | \tilde{\mathcal{M}}_k\right] R_{\psi_c}^2(S_k) + 2\,\mathrm{E}[\lambda_k^I \mu_k^I | \tilde{\mathcal{M}}_k], \\ &= \left[\gamma_k |u_{k,-1}|^2 + (N-\gamma_k)|u_{k,0}|^2\right] \hat{R}_{\psi_c}^2(S_k) \\ &\qquad + \left[(\gamma_k+1)|u_{k,-1}|^2 + (N-\gamma_k-1)|u_{k,0}|^2\right] R_{\psi_c}^2(S_k), \end{aligned} \tag{C.66}$$

$$\begin{aligned} &\mathrm{E}\left[(V_k^I)^2 | \tilde{\mathcal{M}}_k\right]; \\ &\qquad = \left[\gamma_k |v_{k,-1}|^2 + (N-\gamma_k)|v_{k,0}|^2\right] \hat{R}_{\psi_c}^2(S_k) \\ &\qquad\qquad + \left[(\gamma_k+1)|v_{k,-1}|^2 + (N-\gamma_k-1)|v_{k,0}|^2\right] R_{\psi_c}^2(S_k), \end{aligned} \tag{C.67}$$

$$\mathrm{E}\left[(U_k^Q)^2 | \tilde{\mathcal{M}}_k\right] = \mathrm{E}\left[(V_k^I)^2 | \tilde{\mathcal{M}}_k\right], \tag{C.68}$$

$$\mathrm{E}\left[(V_k^Q)^2 | \tilde{\mathcal{M}}_k\right] = \mathrm{E}\left[(U_k^I)^2 | \tilde{\mathcal{M}}_k\right], \tag{C.69}$$

and each pair of random variables in $\left\{U_k^I, V_k^I, U_k^Q, V_k^Q\right\}$ is conditionally uncorrelated given $\mathcal{M}_k$.

From the development above, the $(K-1)$ sets $\left\{W_k^I, W_k^Q\right\}$, $1 \le k \le K-1$ are conditionally uncorrelated given $\mathcal{M}$, and conditioning for $\left\{W_k^I, W_k^Q\right\}$ can be reduced to $\mathcal{M}_k$. From equations

(3.5) and (3.9), both W_k^I and W_k^Q have a conditional mean of zero given $\mathcal{M}_k$. Furthermore,

$$\begin{aligned}
\mathrm{E}\left[(W_k^I)^2|\mathcal{M}_k\right] &= \mathrm{E}\left[(U_k^I)^2|\mathcal{M}_k\right]\cos^2(\Phi_k) \\
&\quad - 2\,\mathrm{E}\left[U_k^I V_k^I|\mathcal{M}_k\right]\cos(\Phi_k)\sin(\Phi_k) + \mathrm{E}\left[(v_k^I)^2|\mathcal{M}_k\right]\sin(\Phi_k) \\
&= \left[\gamma_k|u_{k,-1}|^2 + (N-\gamma_k)|u_{k,0}|^2\right]\hat{R}^2_{\psi_c}(S_k)\cos^2(\Phi_k) \\
&\quad + \left[(\gamma_k+1)|u_{k,-1}|^2 + (N-\gamma_k-1)|u_{k,0}|^2\right]R^2_{\psi_c}(S_k)\cos^2(\Phi_k) \\
&\quad + \left[\gamma_k|v_{k,-1}|^2 + (N-\gamma_k)|v_{k,0}|^2\right]\hat{R}^2_{\psi_c}(S_k)\sin^2(\Phi_k) \\
&\quad + \left[(\gamma_k+1)|v_{k,-1}|^2 + (N-\gamma_k-1)|v_{k,0}|^2\right]R^2_{\psi_c}(S_k)\sin^2(\Phi_k)
\end{aligned} \tag{C.70}$$

Similarly

$$\begin{aligned}
\mathrm{E}\left[(W_k^Q)^2|\mathcal{M}_k\right] &= \left[\gamma_k|v_{k,-1}|^2 + (N-\gamma_k)|v_{k,0}|^2\right]\hat{R}^2_{\psi_c}(S_k)\cos^2(\Phi_k) \\
&\quad + \left[(\gamma_k+1)|v_{k,-1}|^2 + (N-\gamma_k-1)|v_{k,0}|^2\right]R^2_{\psi_c}(S_k)\cos^2(\Phi_k) \\
&\quad + \left[\gamma_k|u_{k,-1}|^2 + (N-\gamma_k)|u_{k,0}|^2\right]\hat{R}^2_{\psi_c}(S_k)\sin^2(\Phi_k) \\
&\quad + \left[(\gamma_k+1)|u_{k,-1}|^2 + (N-\gamma_k-1)|u_{k,0}|^2\right]R^2_{\psi_c}(S_k)\sin^2(\Phi_k)
\end{aligned} \tag{C.71}$$

and

$$\mathrm{E}\left[W_k^I W_k^Q|\mathcal{M}_k\right] = 0. \tag{C.72}$$

Bibliography

[1] M. Pursley, "Performance Evaluation for Phase-Coded Spread-Spectrum Multiple-Access Communication–Part I: System Analysis," *Communications, IEEE Transactions on*, vol. 25, pp. 795–799, Aug 1977.

[2] E. Geraniotis and B. Ghaffari, "Performance of binary and quaternary direct-sequence spread-spectrum multiple-access systems with random signature sequences," *Communications, IEEE Transactions on*, vol. 39, pp. 713–724, May 1991.

[3] J. Holtzman, "A simple, accurate method to calculate spread-spectrum multiple-access error probabilities," *Communications, IEEE Transactions on*, vol. 40, pp. 461–464, Mar 1992.

[4] J. Lehnert and M. Pursley, "Error Probabilities for Binary Direct-Sequence Spread-Spectrum Communications with Random Signature Sequences," *Communications, IEEE Transactions on*, vol. 35, pp. 87–98, Jan 1987.

[5] M. Landolsi and W. Stark, "On the accuracy of Gaussian approximations in the error analysis of DS-CDMA with OQPSK modulation," *Communications, IEEE Transactions on*, vol. 50, pp. 2064–2071, Dec 2002.

[6] M. B. Pursley, *Introduction to Digital Communications*. Upper Saddle River, NJ: Pearson Education, Inc, 2005.

[7] H. Nguyen and E. Shwedyk, "On error probabilities of DS-CDMA systems with arbitrary chip waveforms," *Communications Letters, IEEE*, vol. 5, pp. 78–80, March 2001.

[8] D. Yoon, K. Cho, and J. Lee, "Bit error probability of M-ary quadrature amplitude modulation," in *Vehicular Technology Conference, 2000. IEEE-VTS Fall VTC 2000. 52nd*, vol. 5, pp. 2422–2427 vol.5, 2000.